# *DETERMINATION OF CONTACT PARAMETERS USED IN DEM MODELS FOR REALISTIC SIMULATION OF BALL MILLS*

*A Thesis Submitted*

in Partial Fulfilment of the Requirements

for the Degree of

MASTER OF TECHNOLOGY

*by*

ASUTOSH GOPINATH

*to the*

DEPARTMENT OF MATERIALS & METALLURGICAL ENGINEERING

INDIAN INSTITUTE OF TECHNOLOGY KANPUR

APRIL, 1999

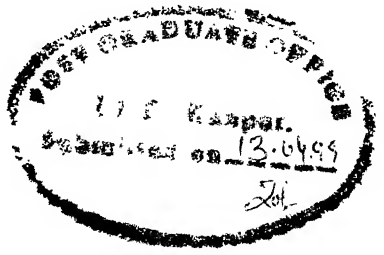


# CERTIFICATE

It is certified that the work contained in this thesis titled "*Determination of Contact Parameters used in DEM Models for Realistic Simulation of Ball Mills*", by *Asutosh Gopinath*, has been carried out under my supervision and that this work has not been submitted elsewhere for a degree.

Date: 13.4.99

Dr. B. K. Mishra,
(Associate Professor),
Materials and Metallurgical Engineering,
Indian Institute of Technology, Kanpur,
April, 1999.

Dedicated to...

my parents

# Acknowledgements

As my academic career at I. I. T. Kanpur is coming to an end with the submission of this thesis, I take the opportunity to express my sincere gratitude to my respected guide Dr. B. K. Mishra for the enlightenment he has bestowed on me about the interesting field of computer simulation. The successful completion of this work has been possible only due to his excellent guidance throughout this work.

I would like to thank all my friends for providing me a cordial and friendly environment and thus making my stay at I.I.T. Kanpur a memorable one.

# Abstract

The discrete element method (DEM) has come a long way in simulating multiple interacting deformable bodies undergoing large absolute or relative motions. These separate bodies can also undergo progressive fracturing and result in the generation of smaller distinct bodies. Therefore, in order to correctly predict the motion and fracture behavior of these distinct elements it is essential to accurately determine the forces developed at the contact points. In the DEM the contact forces are determined by describing the contact behavior through a pair of spring and dashpot. The responses of the spring and the dashpot to any applied external force are the subject of the present investigation so as to make them realistic.

DEM has been used sucessfully to simulate the motion of balls in tumbling mills. While the overall motion of the balls appear to be realistic, a careful look at the corresponding quantitative features such as power draw and impact energy distribution reveal that there is a scope to improve upon the contact model. What is needed is a unified framework within which the contact parameters would be specified such that for any given system these parameters remain insensitive to any change within the system.

In the present work, at first, a bouncing ball problem is considered in detail. The motion of the ball is described by a non-linear differential equation that takes into account a typical spring-dashpot type contact behavior. This equation

is solved numerically to completely describe the motion of the ball before and after the impact. The corresponding experimental work reported in the literature on a very sensitive ultra-fast load cell provided a basis for correlation. Thus, it has become possible to directly extract the contact parameters that are to be embedded in the analytical model. These parameters include the contact stiffness reflecting material and geometric properties of the two contacting surfaces, and the damping coefficient which is a measure of the coefficient of restitution.

In the DEM simulation, identifying the critical time-step is very crucial, as a larger time-step can lead to unrealistic or erroneous results, and a small time-step may give more accurate results but requires large computer memory and a long simulation time. It was found that the contact parameters obtained by non-linear model necessitated a small critical time-step. One way of overcoming this large computational effort was examined using the "Equivalent Linearisation" technique. By using this method an equivalent linear model was obtained from the non-linear model and equivalent parameters were calculated. Interestingly, the equivalent contact parameters so obtained required a larger time-step than in the non-linear model, which significantly reduced the overall computational effort.

A comparative investigation of the linear, the non-linear and the equivalent linearized models was done for the bouncing ball problem. It was found that linearized model was more accurate than the linear model and required lesser computational effort than the non-linear model.

In the concluding part of the present work, DEM simulation of a laboratory size tumbling mill is performed to compare the power draw obtained for the three models.

# Contents

# List of Figures

# List of Tables

# List of Symbols

## Roman Symbols

| | |
|---|---|
| $A$ | Cross section area of bar, $m^2$ |
| $a$ | Tsuji's damping factor |
| $c_o$ | Velocity of strain wave propagation, $msec^{-1}$ |
| $d$ | Diameter of ball, $m$ |
| $E$ | Error in approximation |
| $E_s$ | Young's modulus of sphere, $Nm^{-2}$ |
| $E_w$ | Young's modulus of wall, $Nm^{-2}$ |
| $e$ | Coefficient of restitution |
| $F_{spring}$ | Spring force, $N$ |
| $F_{damping}$ | Damping force, $N$ |
| $f$ | Penetration factor |
| $g$ | Accelaration due to gravity, $msec^{-1}$ |
| $k$ | Non-linear contact stiffness , $Nm^{-1.6}$ |
| $k_{eq}$ | Equivalent contact stiffness, $Nm^{-1}$ |
| $m$ | Mass of object, $kg$ |
| $q$ | Non-linear damping coefficient, $Nm^{-1.8}sec$ |
| $q_{eq}$ | Equivalent Damping coefficient, $Nm^{-1}sec$ |

| | |
|---|---|
| $r$ | Nonlinearity in spring |
| $r_s$ | Radius of sphere, $m$ |
| $s$ | Nonlinearity in dashpot |
| $T$ | Time period of oscillation, $sec$ |
| $t$ | Instantaneous time, $sec$ |
| $v_a$ | Velocity of ball just after impact, $msec^{-1}$ |
| $v_b$ | Velocity of ball just before impact, $msec^{-1}$ |
| $v_o$ | Maximum particle velocity, $msec^{-1}$ |
| $x$ | Particle displacement, $m$ |
| $\dot{x}$ | Particle velocity, $msec^{-1}$ |
| $\ddot{x}$ | Particle accelaration, $msec^{-2}$ |
| $Y$ | Elastic modulus of bar, $Nm^{-2}$ |

# Greek Symbols

| | |
|---|---|
| $\alpha$ | Particle overlap, $m$ |
| $\alpha_{max}$ | Maximum overlap, $m$ |
| $\epsilon$ | Perturbation parameter |
| $\zeta$ | Tsuji's damping term |
| $\mu$ | Coefficient of friction |
| $\nu_s$ | Poisson ratio of sphere |
| $\nu_w$ | Poisson ratio of wall |
| $\rho$ | Density of bar, $kgm^{-3}$ |
| $\omega$ | Angular speed, $radian\, sec^{-1}$ |

# Chapter 1

# Introduction and Literature Review

Discrete element method (DEM) is a computational technique to simulate the behavior of any system comprising discrete interacting particles. In this method, the contact forces acting between particles are represented by a pair of spring and dashpot. For any two or more interacting particles within the system, one pair of spring and dashpot is activated for each contact when the distance between the centre of particles become less than sum of their radii. The contact forces and other body forces are summed to determine the net force acting on a given particle. Then the net acceleration of the particle is determined by using Newton's second law of motion. The positions of the particles are then determined using an explicit numerical time integration recipe such as

$$\dot{x}_{t+\Delta t} = \dot{x}_t + \ddot{x}_t \Delta t \tag{1.1}$$

$$x_{t+\Delta t} = x_t + (\dot{x}_t + \dot{x}_{t+\Delta t})\, 0.5 \Delta t \tag{1.2}$$

Thus, this numerical scheme allows simulation of discretely interacting bodies in an explicit manner that has a wide range of engineering applications.

The DEM that describes the motion of assemblies of particles was pioneered by

Cundall and Strack [1]. Cundall and Strack proposed a model consisting of spring, dashpot and slider components at contact points of adjacent particles. This model is commonly used for calculating the particle impact force which is then used for updating the particle position. Several assumptions about the spring and damping forces used in impact calculations have been made by different researchers. Until few years back linear spring and dashpot model was used to represent a contact, but lately it has been found that a nonlinear spring and dashpot model gives more accurate results [2]. The accuracy of simulation also depends on the accurate determination of contact parameters which facilitate a better estimate of the inter-elemental forces.

The representation of contact as a pair of spring and dashpot has enabled DEM to explore those areas in which interactions between discrete particles of various size and shapes is taking place. Over the past two decades extensive research on DEM has been carried out and it has been successfully applied to simulate discrete particle interactions in many areas. Table 1.1 [3] outlines the areas of application of discrete element method.

In many DEM applications in general, and in ball mill in particular, it has been found that the material parameters selected to simulate spring and dashpot play the most critical role. Even a slight variation in the value of material parameters is likely to give a large variation in the simulation results. Therefore, when DEM is used to predict the power draft of a ball mill which is considered to be a good performance indicator, it is imperative that the parameters are determined carefully. These parameters essentially embody the properties of the system: stiffness, damping, and friction. The contact is typically represented by a system of spring and dashpot as shown in Figure 1.1. The forces in the spring and the dashpot as a result of the contact is determined by the associated stiffness and damping quantities. In the following few paragraphs a brief description on work done by

Table 1.1: Areas of application of the discrete element method.

| Application Areas |
|---|
| •Mineral processing<br>- Simulation of ball-charge motion in tumbling mills<br>- Simulation of bed stratification in jigs |
| • Behavior of soils, rocks and granular materials<br>- Rock pit slope stability behavior<br>- Underground structure stability in jointed rocks<br>- Study of earthquake mechanism and plate tectonics<br>- Modeling of geological structure evolution and formation of reservoir traps<br>- Liquification under dynamic loading<br>- Blast survivability studies<br>- Hazardous waste disposal studies |
| • Impact and explosive dynamics<br>- Automobile crash simulation<br>- Projectile penetration and explosive containment<br>- Kinetic energy weapon effects<br>- Vulnerability and particle tracking studies during explosive fragmentation |
| • Mechanical behavior<br>- Metal forming<br>- Interaction of machinery components<br>- Analysis of linkages and chains<br>- Vibration control and feedback studies<br>- Fracture mechanics<br>- Study of joints and limbs |

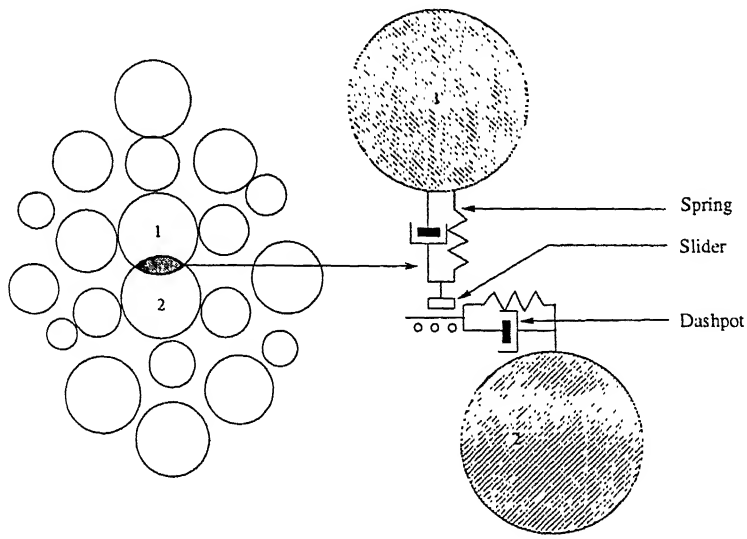


Figure 1.1: Particle contact model (disk-disk contact).

various researchers in modeling the contact and the various ways of determining the contact parameters is presented.

There are basically four types of force-displacements relationships that are used to describe the contact behavior [2]. These relationships and the associated methods for determining the contact parameters are described below:

- Linear contact law is the simplest one in which the contact parameters are independent of the history of contact forces and are typically represented as

$$F_{spring} = kx \tag{1.3}$$

$$F_{dashpot} = q\dot{x} \tag{1.4}$$

where, $k$ is the stiffness parameter and $q$ is the viscous damping coefficient. The spring and dashpot are simply placed between the contacting particles to simulate the load-displacement responses. Since the contact parameters are assumed to be constant, this law fails to simulate the pressure-dependency

of parameters of the medium and thus is not realistic.

- Non-linear contact law is the second method for determining contact parameters. In this method, a non-linear representation of contact force is done. The contact parameters are represented as

$$F_{spring} = kx^r \tag{1.5}$$

$$F_{dashpot} = qx^s\dot{x} \tag{1.6}$$

where $r$ is the non-linearity in spring and $s$ is the non-linearity in dashpot. The contact parameters are determined by using Mindlin solution for contact. For the case of identical elastic rough spheres of radius $r_s$ and elastic constants $E_s$ and $\nu_s$, the normal stiffness $k$ can be written as

$$k = \frac{2E_sA}{(1-\nu_s)} \tag{1.7}$$

where $A$ is the radius of contact area. The tangential stiffness, on the other hand, depends upon the complete history of normal and shear forces. This law gives a more realistic simulation but requires large computational time and memory.

- Modified linear contact law was proposed to save computer time and memory, and to avoid the complication of Mindlin solution. In this method, the normal stiffness was taken same as in Mindlin solution, but the shear contact stiffness was made a linear function of current normal force acting at the contact. This aided in doing away with the cumbersome task of determine the complete history of normal and shear forces which might vary from sys-

tem to system. The main limitation of the law is for cyclic load simulation, where it does not predict the realistic behavior of contact.

- Modified non-linear contact law was proposed to reduce the computational time and memory requirement. In this method, the normal stiffness is the Mindlin stiffness give by Eq. 1.7, and the shear stiffness is some non-linear function of the current value of normal and tangential contact forces.

The four contact laws outlined above serve as a basis for modeling contacts in various discrete particle systems. Quite a few models have been developed either directly using the above laws or by slightly modifying them. The following sections deals with work done in modeling system comprising discrete particles using the above mentioned contact laws.

## 1.1 Contact Force Analysis for Spring Dashpot Models

The linear contact model was first used by Cundall and Strack [1]. This is the most commonly used model that assumes a linear spring and a linear damper. The force is applied when the particles overlap, that is when the distance between their centres is less than the sum of the particle radii. For a linear spring and dashpot, the equation of motion of an impacting particle can be expressed as:

$$m\ddot{\alpha} + q\dot{\alpha} + k\alpha = 0 \tag{1.8}$$

where $m$ is the mass of ball, $\alpha$ is the particle overlap, $q$ is the damping coefficient, and $k$ is the contact stiffness.

In order to determine contact stiffness, Zhang *et al* [4] limited the maximum

anticipated inter-particle penetration, $\alpha_{max}$, to be a small fraction of the particle diameter $d$. This constraint was achieved by defining:

$$k = f^2 m v_o^2 / d^2 \tag{1.9}$$

where $v_o$ is the anticipated maximum speed of any particle in the system, and $f$ is the penetration factor defined by putting $\alpha_{max}$ equal to $d/f$ In this study the value of $f$ was chosen to be equal to 10.0. The damping coefficient $q$ was defined by:

$$q = 2 \ln (1/e) \left[ \frac{k m_i m_j / (m_i + m_j)}{\pi^2 + (\ln (1/e))^2} \right]^{1/2} \tag{1.10}$$

where $k$ is the contact stiffness, and $m_i$ and $m_j$ are the masses of the disks $i$ and $j$ respectively.

For the discrete particle simulation of two-dimensional fluidized bed, Tsuji *et al* [5] used the linear model by assuming a constant value for stiffness. Qualitatively, the results were satisfactory in many respects, such as particle circulating motion and mixing, but the model could not predict the correct force versus time trend (Figure 1.2).

Experiments carried out by Zhang and Whiten [6] have shown that the expression for damping is incorrect, and added that the damping coefficient $q$ should not be constant, but is expected to be a function of displacement. They showed (Figure1.3) that when the damping is non-zero, the initial force is large, which is contrary to experimental measurements that show the force rising smoothly from zero to maximum value and then returning smoothly to zero.

Over the last few years, quite a few papers have been published by different researchers reporting modeling of contact force by non-linear spring and dashpot.

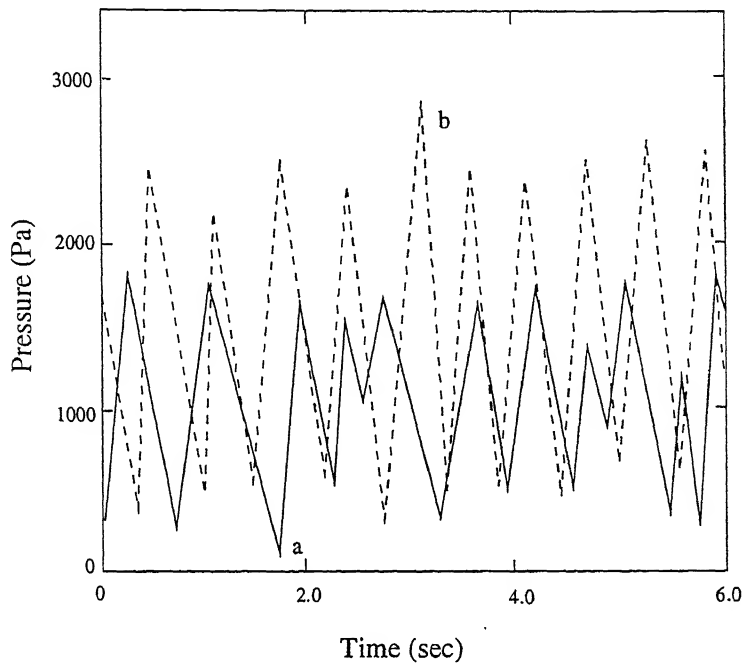


Figure 1.2: Pressure fluctuation: (a) experiment; (b) calculation [5].

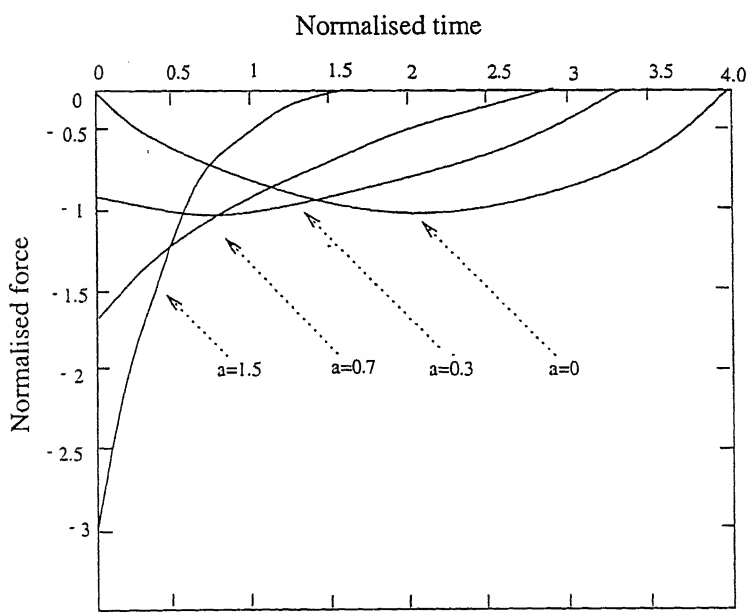


Figure 1.3: Normalized force verses normalized time using linear model, $a$ is normalized damping [6].

The non-linear impact phenomenon was first and extensively studied by Hertz. For linearly elastic and homogeneous, with perfectly smooth contact surfaces, Hertz [7] calculated that the force acting at the contact area (known as Hertz spring force) using:

$$F_{spring} = k\alpha^{3/2} \tag{1.11}$$

where $k$ is the material stiffness and $\alpha$ is the elastic approach of the colliding bodies. Hence, the equation of motion of head-on colliding bodies can be written as:

$$m\ddot{\alpha} + k\alpha^{3/2} = 0 \tag{1.12}$$

where, $m$ is the mass of body.

It was experimentally proved by Velusami [7] that a contact damping force also existed at the impact area. According to him, the damping force is given by $F_{damping} = q\alpha^{3/2}\dot{\alpha}$ so, the equation of motion of the impacting body can be written as:

$$m\ddot{\alpha} + q\alpha^{3/2}\dot{\alpha} + k\alpha^{3/2} = 0 \tag{1.13}$$

where, $q$ is the damping constant.

Hertz theory is limited to metal-metal impact only. Realizing the implication of Hertz's analysis, researchers in the field of DEM applied non-linear force theory to obtain a more realistic model for contact force. Yet another non-linear model came up, but this time by Tsuji *et al* [8]. But the model used to represent damping differed greatly with that of Velusami. Here the the damping coefficient was found heuristically and was taken as $\zeta = a(mk)^{1/2}\alpha^{1/4}$. The equation of motion was

written as

$$m\ddot{\alpha} + \zeta\dot{\alpha} + k\alpha^{3/2} = 0 \tag{1.14}$$

or,

$$m\ddot{\alpha} + a(mk)^{1/2}\alpha^{1/4}\dot{\alpha} + k\alpha^{3/2} = 0 \tag{1.15}$$

where, $a$ is a constant which depends on coefficient of restitution $e$.

The contact stiffness $k$ was determined by contact theory. In the case of two spheres of same size (radius equal to $r_s$), $k$ is expressed by:

$$k = \frac{\sqrt{2r_s}E_s}{3(1-\nu_s^2)} \tag{1.16}$$

where, $E_s$ is the Young's modulus, and $\nu_s$ is the Poisson ratio of the particles. In case of contact between a sphere and a wall, $k$ is expressed by:

$$k = \frac{\frac{4\sqrt{r_s}}{3}}{\frac{1-\nu_s^2}{E_s} + \frac{1-\nu_w^2}{E_w}} \tag{1.17}$$

where, $E_w$ is the Young's modulus, and $\nu_w$ is the Poisson ratio of the wall. Tsuji *et al* used the above non-linear model to simulate the plug flow of cohesionless particles in a horizontal pipe [8]. This model however showed marked quantitative disagreement with experiment, but was satisfactory in the sense that the method needed fewer empirical factors than the existing analyses of plug flow.

Goldsmith [9] came up with another non-linear model using the theory of compressive strain wave propagation in solid, that described the motion of a high-

speed impact of an elastic sphere on the end of a uniform bar as:

$$m\ddot{\alpha} + \frac{3}{2}\frac{mk}{\rho A c_o}\alpha^{1/2}\dot{\alpha} + k\alpha^{3/2} - mg = 0 \tag{1.18}$$

where, $g$ is the acceleration due to gravity, $\rho$ is the density of bar, $A$ is the cross-section area of bar, $c_o = \left(\frac{Y}{\rho}\right)$ is the velocity of propagation of strain wave down the bar, and $Y$ is the elastic modulus of bar.

King and Bourgeois [10] used this model to simulate the energy required for particle breakage. The diameter of rod was 3/4 inch, the diameter and mass of ball used were 1 inch and 0.067 kg, respectively. The expression for $k$ used here was same as that used by Tsuji *et al* [8] for ball-wall impact. Again, in this case, quantitative disagreement regarding variation of contact force versus time was observed ( Figure 1.4).

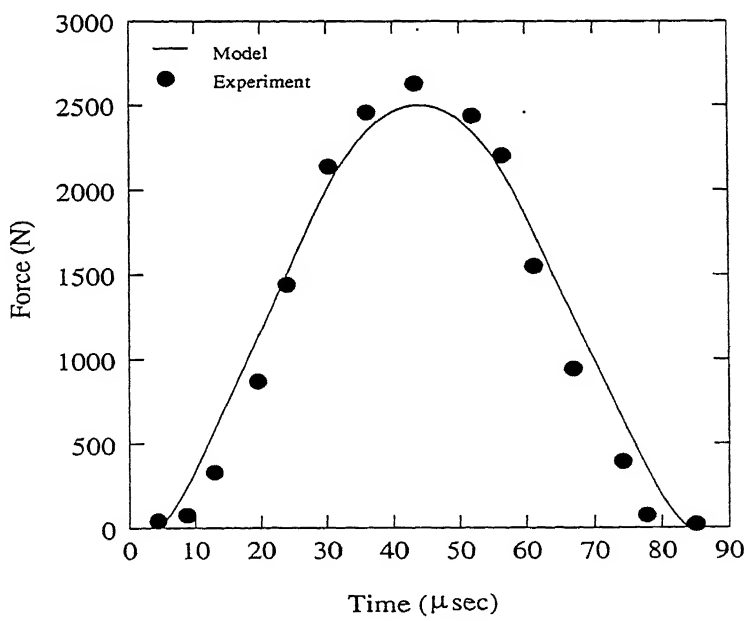


Figure 1.4: Comparison of predicted and measured responses from 5 $cm$ drop height [10].

## 1.2 Limitations of Earlier Works

For simulation of a ball mill, a detailed study of the parameters involved in the process of grinding is necessary. The most important parameters from the point of view of power requirement during grinding are stiffness and damping. All the models outlined in this chapter are purely theoretical and are heavily based on certain assumptions that might drastically affect their performance when they are directly applied to simulate the behavior of ball-charge motion in industrial mills.

The assumptions which these models make are given below:

- In all the above models, the damping term is assumed to be a constant independent of the amount of deformation undergone by the particles. This results in erroneous calculation of contact forces [6]. Initially, just prior to contact the damping force should be zero and then it should change gradually. Tsuji's model, on the other hand, is able to do this qualitatively but quantitatively it requires some more adjustment. Also, Tsuji's and Goldsmith's model is inefficient in predicting force-displacement history which is very important because it gives an idea about energy loss of the system.

- Since the DEM deals with individual particles with normal and shear contact springs and dashpots, it is not possible to specify overall aggregate properties as the Young's modulus, coefficient of friction, coefficient of restitution, and Poisson ratio. Instead, it is necessary to choose approximate values of contact parameters [12]. The quantitative discrepancies in the results obtained by various researchers can be attributed to this.

## 1.3 Scope of Present Work

In the present work, instead of using the contact parameters that were obtained theoretically by researchers, an attempt has been made, for the first time, to extract the relevant parameters by correlating the model developed with the experimentally obtained data. This makes the present work more realistic in the sense that a model is developed by analysis of experimental data obtained from literature [13, 14]. By doing this certain assumptions pertaining to material characteristics, *e.g.* smooth surface and no prior deformation are done away with. Secondly, the damping term is modeled in such a way that the unrealistically high initial force is suppressed and quantitative agreement with experiment is achieved. Finally, average values of contact parameters which are obtained by using the model developed in present work, for different mill conditions, are selected for simulation of power draw of a laboratory size ball mill. This ensures incorporation of individual contact characteristics to gross ball-charge behavior.

# Chapter 2

# Determination of Contact Stiffness and Damping

In this chapter, a vast amount of experimental data on single ball impact are analyzed. The force- displacement as well as the force-time relationship during a collision is considered. These experimental data are fitted to a non-linear spring-dashpot model of the following form

$$m\ddot{\alpha} + q\alpha^s\dot{\alpha} + k\alpha^r = 0 \tag{2.1}$$

where $k$ is the stiffness parameter which determines the maximum force attained during impact, $r$ is the nonlinearity in the spring, $q$ is the damping parameter which determines the amount of energy expended during the impact, and $s$ is a measure of the non-linearity in the dashpot. Different values for the parameters were assumed and the best values were selected that matched the experimental data. The data were obtained by conducting drop-ball tests [13] on ultra fast load cell device.

## 2.1 Drop-Ball Test

In order to determine the most realistic values of the contact parameters, an elaborate analysis of numerous experimental data gathered by means of the ultrafast load cell equipment [13] ($UFLC$) was carried out. The description of $UFLC$ is given in the following section.

## 2.2 Description of Ultrafast Load Cell Device

Ultrafast load cell (UFLC) device is a device to measure impact responses of materials under dynamic loading conditions. The loading and fracture of particles in tumbling mills happens within a very short period of time. With UFLC, the grinding action can be studied in detail by measuring the impact of a ball dropping into a bed of mineral particles. The UFLC has a resolution of $10^{-5}$ second.

In this apparatus, a drop-weight impacts from a certain height on a particulate agglomerate situated on top of a steel rod. The sphere release mechanism can be adjusted vertically to vary the drop height of the impacting sphere. The UFLC utilizes the propagation of elastic waves. The impact of drop-weight on particles results in a pressure on top of the rod which causes a compressive strain wave to propagate through the rod. This strain wave is detected by solid state strain gauges which are glued to the rod. The signal from the strain gauges is amplified and stored in a digital storage oscilloscope which is interfaced to a computer. From the recorded wave, the force acting on the particle is computed. A schematic of this equipment is drawn in Figure 2.1.

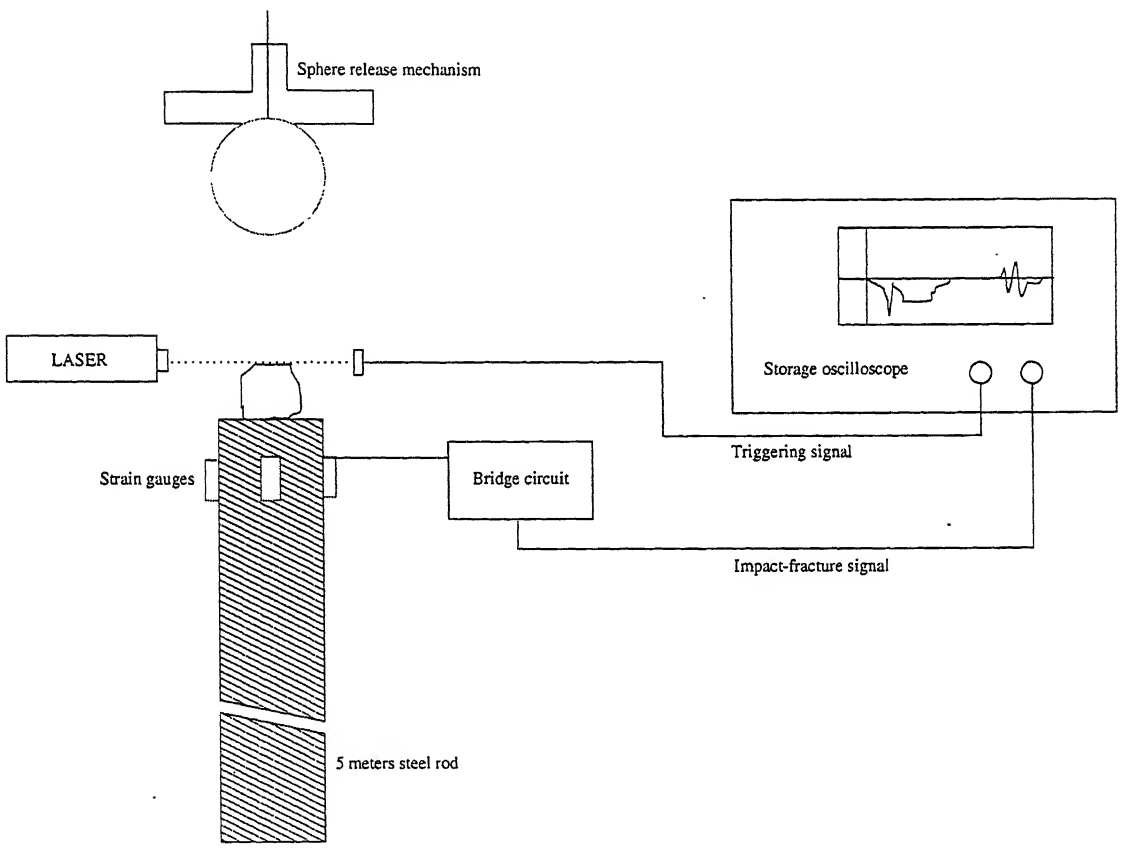


Figure 2.1: Schematic outline of the ultra-fast load cell.

## 2.3 Experimental Data on UFLC

A series of drop-ball tests were carried out by Höfler [13] and Mishra [14] at the Comminution Center of the University of Utah. Two types of data were gathered from drop-ball tests: first, impacts in which there was no particle layer laid on the rod, *i.e.*, the ball was directly dropped on the rod, and second, impacts in which there were one or more layers of particles laid on the rod. One type of data is useful because it represents the metallic collisions of ball-ball and ball-wall type in a ball mill, and the other type of data is useful for the determination of parameters to simulate material breakage in ball mill. For metal-metal impact with no particle layers in between, three balls of mass 0.096, 0.252 and $0.647\,kg$ were dropped from a height of $0.3\,m$. The force-time and force-deformation history on the top surface of ultra fast load cell rod was detected by the solid state strain gauges and recorded in the oscilloscope. Whereas, the other type of data was obtained by conducting experiments for different drop-heights, number of particle layers, masses of the impacting ball and types of material placed between the impacting bodies. In this case the maximum force developed at the contact and energy loss due to impact were recorded. The experimental data is presented in Appendix A in Table A.1 through Table A.4.

In this chapter, a methodology is developed to extract the contact parameters from the data obtained by means of drop ball tests.

## 2.4 Determination of Contact Parameters for Metal-Metal Impact

The contact parameters were determined by solving the model equation (Eqn. 2.1) in two steps. First, the range of nonlinear parameters $r$ and $s$ were fixed. The

nonlinearity in the spring $r$ was kept in the range $1-2$. Similarly, the nonlinearity in dashpot $s$ was kept in the range $0-1$. Second, approximate values of contact parameters $k$ and $q$ were taken as initial guess values. Then the model equation was solved using Fourth Order Runge-Kutta method. The force-displacement and force-time relationship fitted with the corresponding experimental results. In case of any mismatch, the values of all the model parameters were modified and the procedure was repeated all over again. The results showing force-time and force-deformation history both for the model and experiment in case of metal-metal impacts are shown in Figure 2.2 through Figure 2.4.

It was found that the predicted result matched the experimental data in all three cases for $r$ equal to 1.6 and $s$ equal to 0.8. However, the numerical values of $k$ and $q$ varied in each case. Table 2.1 summerises the experimental conditions and the corresponding numerical results. The values of stiffness $k$ and damping $q$ obtained numerically were used to calculate the energy loss due to metal-metal impact. The energy loss was obtained by calculating the area enclosed by force-deformation loop. The energy of impact obtained by using $k$ and $q$ that are extracted from the non-linear model were in good agreement with the measured energy for different ball masses. Thus, for the metal-metal impact the model took the following form:

$$m\ddot{\alpha} + q\alpha^{0.8}\dot{\alpha} + k\alpha^{1.6} = 0 \tag{2.2}$$

This analysis however, points to the fact that a linear contact model is not appropriate inasmuch as it fails to predict the force-time Figure 1.3 history. However, with proper tuning of the parameters, the impact energy can be matched for a given collision. Although non-linear models can predict the force-time history during a collision as seen here, the associated parameters turn out to be numer-

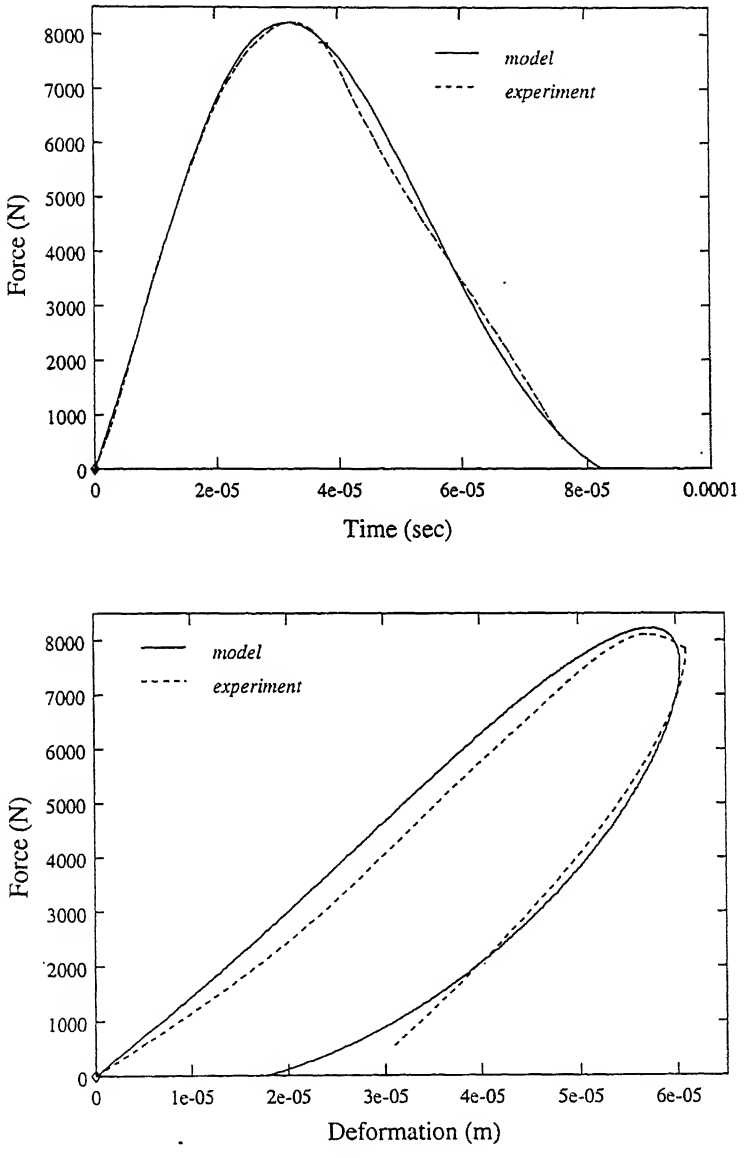


Figure 2.2: Comparison between experiment [14] and model for ball-flat impact for ball of mass 0.096 kg.

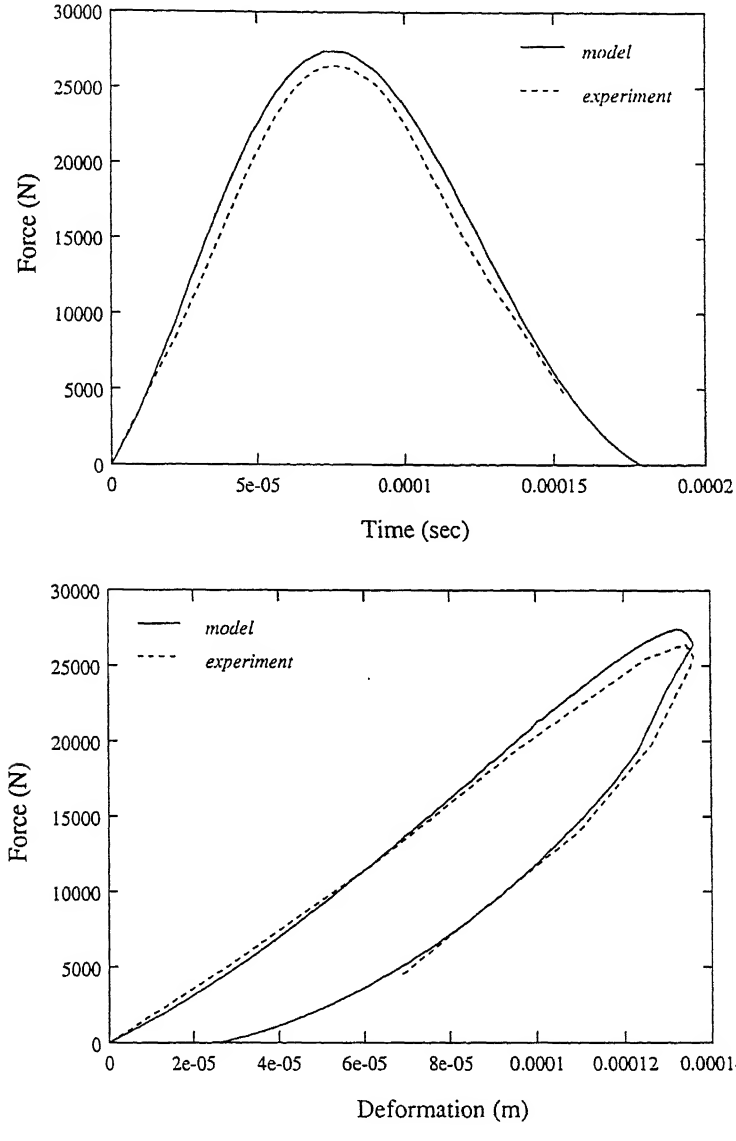


Figure 2.3: Comparison between experiment [14] and model for ball-flat impact for ball of mass 0.647 kg.

Table 2.1: $k$ and $q$ values and comparisons between model and experimental [14] energy loss for metal-metal impact.

| Experiment No. | 1 | 2 | 3 |
|---|---|---|---|
| Ball mass $(kg)$ | 0.096 | 0.647 | 0.252 |
| Non-linear stiffness $k$ | 4.8e10 | 5.2e10 | 5.0e10 |
| Non-linear damping $q$ | 4.5e6 | 4.9e6 | 4.8e6 |
| Energy loss model $(J)$ | 0.187 | 0.985 | 0.454 |
| Energy loss Experimental $(J)$ | 0.20 | 1.08 | 0.47 |
| Absolute error (%) | 6.5 | 8.8 | 3.4 |

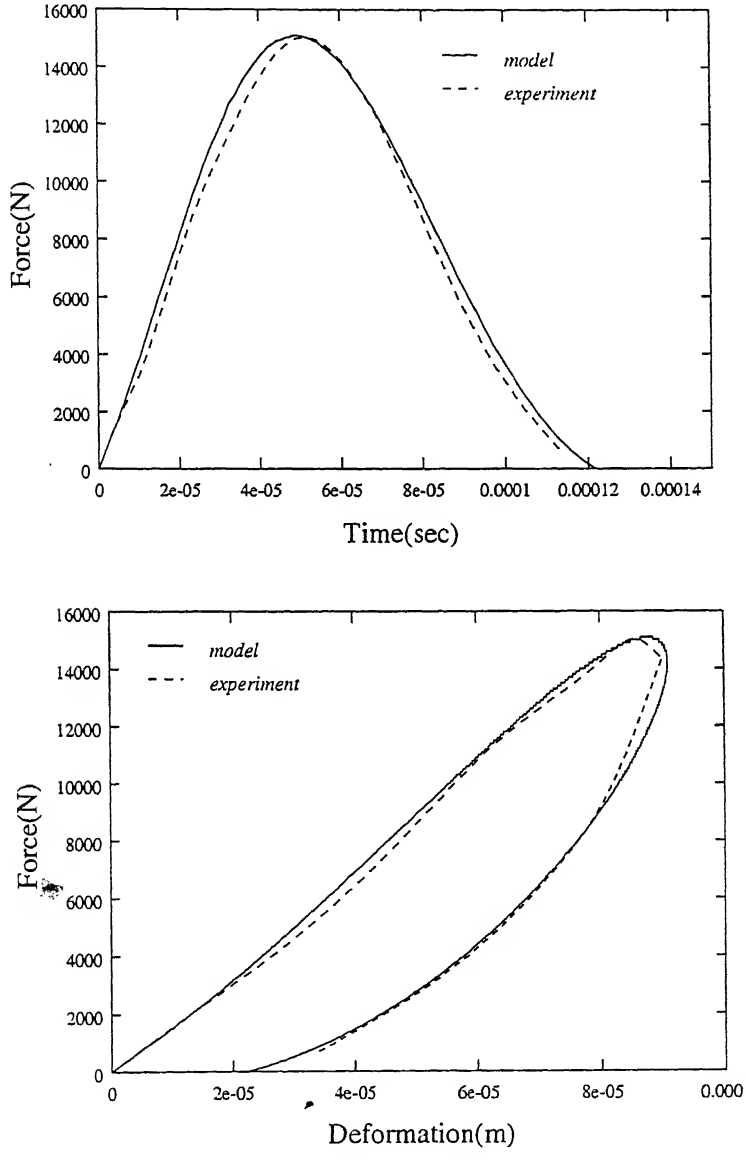


Figure 2.4: Comparison between experiment [14] and model for ball-flat impact for ball of mass 0.252 kg.

ically large. For example, as seen from Table 2.1, the non-linear stiffness values are on an average of the order of $10^{10}$. This turns out to be the most significant drawback of employing a non-linear contact model in the discrete element method. This aspect is discussed in section 2.5 below.

## 2.5 Constraint of Critical Time-step

Consider a body of mass $m$ suspended from a rigid support by a spring of stiffness $k$. The mass is made to oscillate simple harmonically. The time period $\Delta t$ (or critical time-step) of its oscillation can be shown to be equal to

$$\Delta t = 2\sqrt{m/k} \tag{2.3}$$

In order to accurately estimate the motion of particles using DEM, where each contact is represented by a pair of oscillating spring and dashpot, the time-step chosen is 1/10 smaller than the critical time-step. This is done to accurately capture the motion of the impacting balls. Hence, in problems involving simulation by discrete element method, the critical time-step is given by

$$\Delta t = 0.2\sqrt{m/k} \tag{2.4}$$

where $m$ is the mass of the smallest ball. As it is clear that for very large value of $k$ obtained by non-linear model, the critical time-step becomes very small. Therefore, such a large value of $k$ would require calculations of order $10^{10}$ for each ball in 1 second of real time. Therefore, it would require huge memory space and very long simulation time.

The computational constraint of large memory space and time requirements

relieved if the value of $k$ is of a lower order. It has been observed that for the linear model, the computational time requirement is quite less, but at the same time it does not correctly predict force-time and force-deformation histories. This discrepancy of the linear model propagates into the DEM algorithm resulting in erroneous calculation of energy loss. Hence, in the present work, a linear model was obtained from the non-linear one in such a way that the error in calculation of energy loss was minimized. In other words, it can be said that the linear model obtained was equivalent to the non-linear model in terms of energy loss prediction. The technique which is employed to get the equivalent values of contact parameters from the non-linear model by converting it into equivalent linearized form is known as "Equivalent Linearisation" and is described in the following section.

## 2.6 Equivalent Linearisation

Consider the non-linear equation of the form:

$$\ddot{x} + \epsilon f(x, \dot{x}) = F(t, T) \tag{2.5}$$

where $\epsilon$ is the perturbation parameter and $T$ is the time period. This equation can be approximated by:

$$\ddot{x} + \beta_{eq}\dot{x} + \kappa_{eq}x = F(t, T) \tag{2.6}$$

and the error $E$ in the approximation is:

$$E(x, \dot{x}) = [\epsilon f(x, \dot{x}) - \kappa_{eq}x - \beta_{eq}\dot{x}] \tag{2.7}$$

The average of the square of the error over one cycle is:

$$\left\langle E^2(x,\dot{x})\right\rangle_T = \frac{1}{T}\int_0^T [\epsilon f(x,\dot{x}) - \kappa_{eq}x - \beta_{eq}\dot{x}]^2 dt \tag{2.8}$$

Minimizing this quantity with respect to the coefficients $\kappa_{eq}$ and $\beta_{eq}$,

$$\frac{\partial}{\partial \kappa_{eq}}\left\langle E^2\right\rangle_T = -\frac{1}{T}\int_0^T xE dt = 0 \tag{2.9}$$

and,

$$\frac{\partial}{\partial \beta_{eq}}\left\langle E^2\right\rangle_T = -\frac{1}{T}\int_0^T \dot{x}E dt = 0 \tag{2.10}$$

$$\Rightarrow \qquad \int_0^T x[\epsilon f(x,\dot{x}) - \kappa_{eq}x - \beta_{eq}\dot{x}]dt = 0 \tag{2.11}$$

Therefore,

$$\int_0^T \epsilon x f(x,\dot{x})dt - \int_0^T \kappa_{eq}x^2 dt - \int_0^T \beta_{eq}x\dot{x}dt = 0 \tag{2.12}$$

Since, $\int_0^T x\dot{x}dt \equiv 0$ for a periodic solution,

$$\kappa_{eq} = \frac{\int_0^T \epsilon x f(x,\dot{x})dt}{\int_0^T x^2 dt} \tag{2.13}$$

Similarly,

$$\beta_{eq} = \frac{\int_0^T \epsilon \dot{x} f(x,\dot{x})dt}{\int_0^T \dot{x}^2 dt} \tag{2.14}$$

Having minimized the error, it is then neglected. Hence, the governing non-linear

equation reduces to an equivalent linear equation:

$$\ddot{x} + \beta_{eq}\dot{x} + \kappa_{eq}x = F(t,T) \tag{2.15}$$

Note that both $\beta_{eq}$ and $\kappa_{eq}$ depend on the solution $x(t)$. Also, the signs of $\frac{\partial^2}{\partial\kappa_{eq}^2}\langle E^2\rangle$, $\frac{\partial^2}{\partial\kappa_{eq}\beta_{eq}}\langle E^2\rangle$ and $\frac{\partial^2}{\partial\beta_{eq}^2}\langle E^2\rangle$ indicate that by setting the quantities $\frac{\partial}{\partial\kappa_{eq}}\langle E^2\rangle$ and $\frac{\partial}{\partial\beta_{eq}}\langle E^2\rangle$ to zero, $E^2$ is minimized. The equivalent linearisation method is most suited for systems with small non-linearities. However, it is applied for ball-ball and ball-wall contact also to explore its applicability, even though the non-linearities in these cases are much more severe.

Thus, the non-linear model

$$m\ddot{\alpha} + q\alpha^{0.8}\dot{\alpha} + k\alpha^{1.6} = 0 \tag{2.16}$$

on equivalent linearisation is transformed into

$$m\ddot{\alpha} + q_{eq}\dot{\alpha} + k_{eq}\alpha = 0 \tag{2.17}$$

where, $q_{eq}$ is the linearized viscous damping coefficient, and $k_{eq}$ is the linearized stiffness term. Hence,

$$k_{eq} = \frac{\int_0^T \alpha f(\alpha,\dot{\alpha})dt}{\int_0^T \alpha^2 dt} \tag{2.18}$$

and,

$$q_{eq} = \frac{\int_0^T \dot{\alpha} f(\alpha,\dot{\alpha})dt}{\int_0^T \dot{\alpha}^2 dt} \tag{2.19}$$

Thus, for metal-metal impact, the different models investigated in this study are

presented below

$$Linear\,model \;:\; m\ddot{\alpha} + q_{lin}\dot{\alpha} + k_{lin}\alpha = 0 \qquad (2.20)$$

$$Non-linear\,model \;:\; m\ddot{\alpha} + q\alpha^{0.8}\dot{\alpha} + k\alpha^{1.6} = 0 \qquad (2.21)$$

$$Equivalent-linearised\,model \;:\; m\ddot{\alpha} + q_{eq}\dot{\alpha} + k_{eq}\alpha = 0 \qquad (2.22)$$

Table 2.2 shows the equivalent linearized values of contact parameters $k_{eq}$ and $q_{eq}$ found by the method outlined above and also the predicted energy loss for the case of metal-metal impact. The table also shows the stiffness and damping parameters taken for linear model. In case of linear model the value of stiffness $k_{lin}$ was taken as initial slope of experimental force-displacement curves in Figure 2.2 through Figure 2.4. The damping constant in this case was determined by [16] (for derivation see Appendix B)

$$q_{lin} = -2\ln e\sqrt{\frac{mk_{lin}}{\ln^2 e + \pi^2}} \qquad (2.23)$$

where, $m$ is the ball mass and $e$ is the coefficient of restitution. The value of coefficient of restitution was taken as 0.8.

As seen from Table 2.2, the equivalent linearized parameters give more accurate prediction than linear parameters. It is also observed that the equivalent value of stiffness entails calculation of the order of $10^8$ which is significantly lower than the order $10^{10}$ of stiffness obtained by non-linear model (see Table 2.1). Hence, it can be concluded that equivalent linearized model is a good compromise between linear and non-linear models as far as accuracy and computational time requirement is concerned.

Furthermore, in tumbling mills grinding particles, metal-metal impacts are less likely to occur. More than 90 % of impacts occur in which particle layers are

Table 2.2: $k_{eq}$ and $q_{eq}$ values and comparisons between linear model, non-linear model, equivalent linearized model and experimental energy losses for metal-metal impact.

| Experiment No. | 1 | 2 | 3 |
|---|---|---|---|
| Ball mass $(Kg)$ | 0.096 | 0.647 | 0.252 |
| Linear stiffness $k_{lin}$ | 1.4e8 | 1.26e8 | 1.35e8 |
| Linear damping $q_{lin}$ | 519.5 | 1279.4 | 826.5 |
| Equivalent stiffness $k_{eq}$ | 1.17e8 | 1.72e8 | 1.13e8 |
| Equivalent damping $q_{eq}$ | 984.74 | 1912.86 | 1361.34 |
| Energy loss linear model $(J)$ | 0.181 | 0.948 | 0.446 |
| Energy loss non-linear model $(J)$ | 0.187 | 0.985 | 0.454 |
| Energy loss linearized model $(J)$ | 0.185 | 0.967 | 0.451 |
| Energy loss Experimental $(J)$ | 0.20 | 1.08 | 0.47 |
| Absolute error % linear model | 9.5 | 12.2 | 5.1 |
| Absolute error % non-linear model | 6.5 | 8.8 | 3.4 |
| Absolute error % linearized model | 7.5 | 10.5 | 4.04 |

trapped between the balls. Therefore, the contact parameters obtained in this chapter cannot simulate the actual mill condition because they represent metal-metal impact only. Hence, more analysis was done to obtain the parameters in order to simulate the actual mill conditions. The model adopted to analyze the force-time and force-displacement behavior during metal-metal impact was assumed to hold good where the layers of particles are caught in between the impacting bodies. This assumption was necessary because the experimental force-time and force-displacement plots were not available for impacts in which particle layers present between the impacting bodies. This has direct application in ball mill simulation using DEM. Ball mills are used for grinding particles. The tumbling action of the balls impart the required force on the particles. DEM models are used to simulate not only the tumbling actions of the entire ball mass but also the resulting distribution of forces and power draw. It is essential that the parameters in the DEM model be chosen so as to minimize the computational time and accurately predict the power draw.

In order to meet the above objectives it is proposed to represent the impact where layers of particles are caught between the colliding bodies. In other words, it is assumed that a hypothetical layer of particles surrounds the impacting balls as shown in the following schematic (Figure 2.5). This idea is explored to obtain the contact parameters as discussed in Chapter 3.

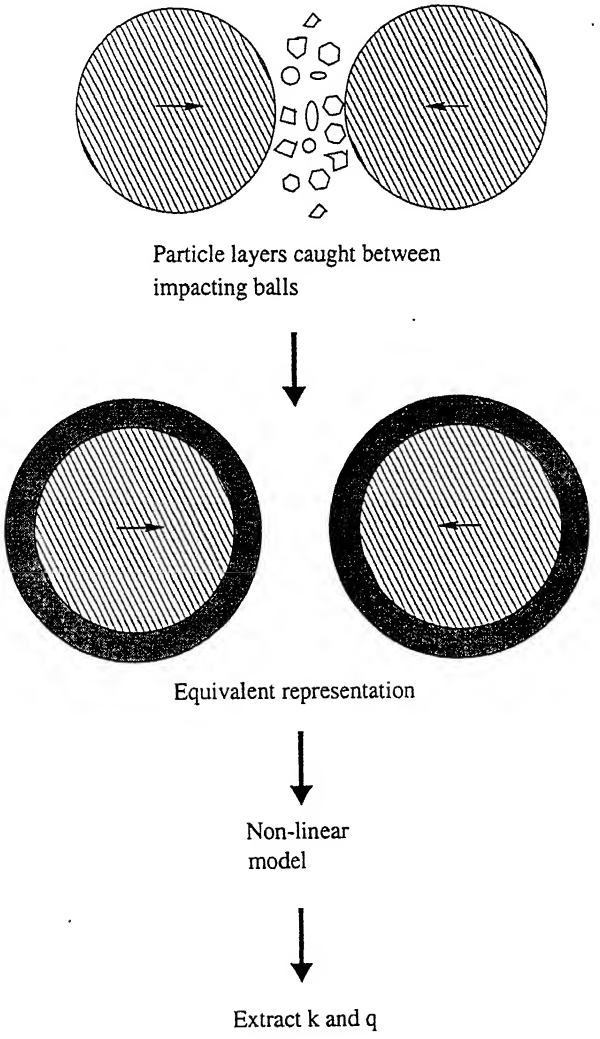


Figure 2.5: A schematic showing hypothetical layer of particles surrounding the impacting balls.

# Chapter 3

# Determination of Contact Parameters for Mill Conditions

Determination of contact parameters under real milling conditions is conceived in a different manner. The earlier approach as described in Chapter 2 is only valid under hypothetical situation where a ball mill is operated without any particles in it. In real mills, particles are ground by the tumbling action of the ball. Therefore, the contact parameters are not exactly the one that would correspond to a metal-metal collision. In this chapter, pertinent experimental data from the literature is collected. These are drop ball test data with layers of particles present between the colliding masses. As before, a non-linear model is fitted to the experimental data and the associated parameters of the model are extracted.

## 3.1 Analysis of Experimental Data

The contact parameters obtained for metal-metal impacts cannot be used for tumbling mills because more than 90 % impacts capture layers of particles. Therefore, in order to obtain the contact parameters it is essential to collect data under con-

ditions that would apply to a ball mill. Höfler [13] did drop ball tests in the UFLC using layers of particles. However, his data (Table A.2 through Table A.4) basically show variations in maximum impact force developed and energy required in breaking particles caught between the balls as a function of drop height, number of particle layers, and material type.

### 3.1.1 Effect of Drop Height on Energy Loss and Impact Force

It is observed that both the impact force and energy loss increase with drop height. The Figure 3.1 and Figure 3.2 depict this effect for particle 5 and 10 layers of particles of quartz. It is also seen that the number of layer has negligible effect on energy loss but it has noticeable effect on maximum force developed on the particles.

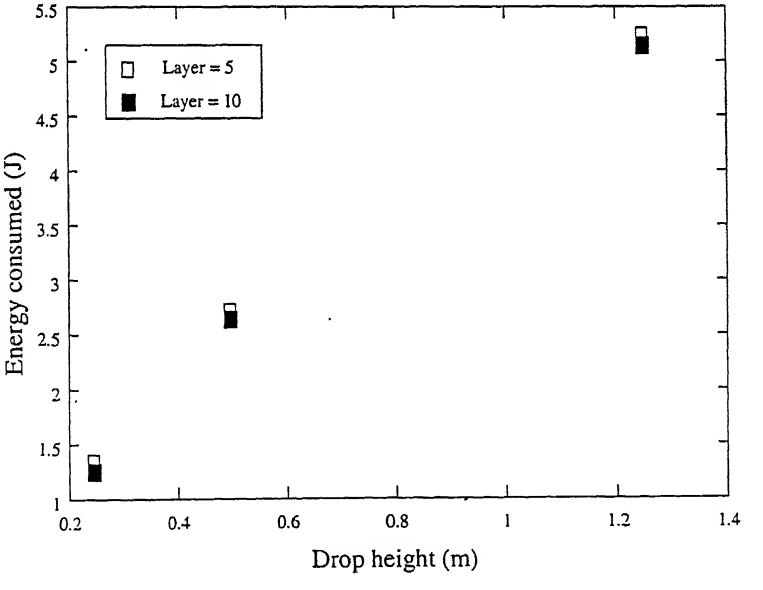


Figure 3.1: Effect of drop height on energy loss due to impact of ball of mass $0.647\,kg$ on layers of quartz [13].

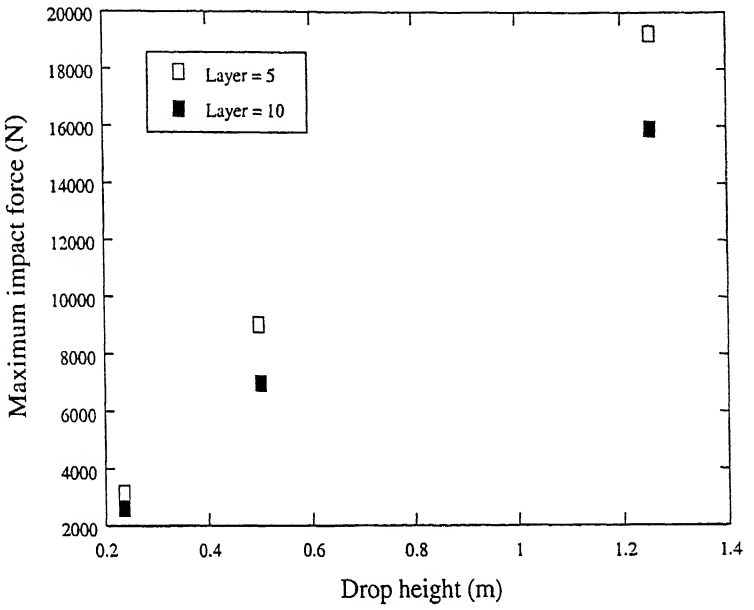


Figure 3.2: Effect of drop height on impact force due to impact of ball of mass $0.647\,kg$ on layers of quartz [13].

### 3.1.2 Effect of Material Type on Energy Loss and Impact Force

It is observed that energy loss increases from quartz to limestone and further to magnetite. The maximum impact force is also found to increase in the same order. Both types of behavior can be attributed to the micro-structural features such as presence of pores, cracks and other flaws in materials. Materials having lower number of flaw per unit volume have higher strength and consequently require higher force to deform and more energy to fracture. Similarly, materials having greater flaw density are brittle and require lower force to deform and lesser energy to fracture (Figure 3.3 and Figure 3.4).

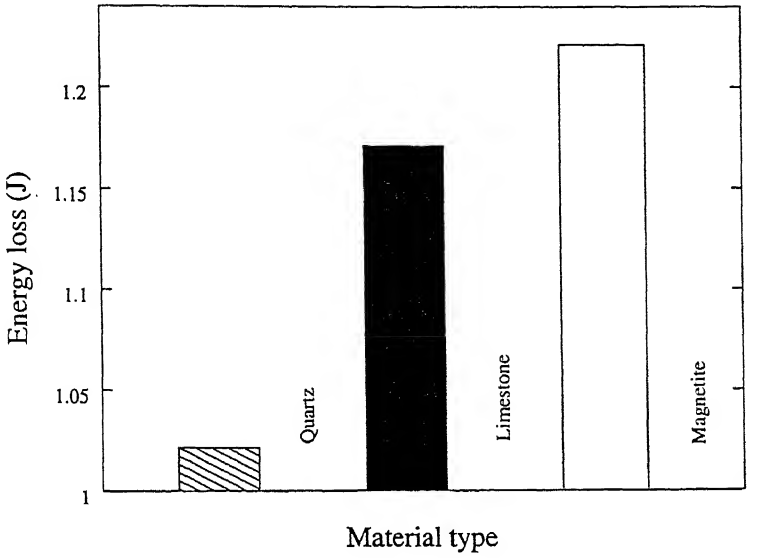


Figure 3.3: Effect of material type on energy loss for ball of mass 0.252 $kg$ dropped from a height of 0.5 $m$ on 2 layers of particles [13].

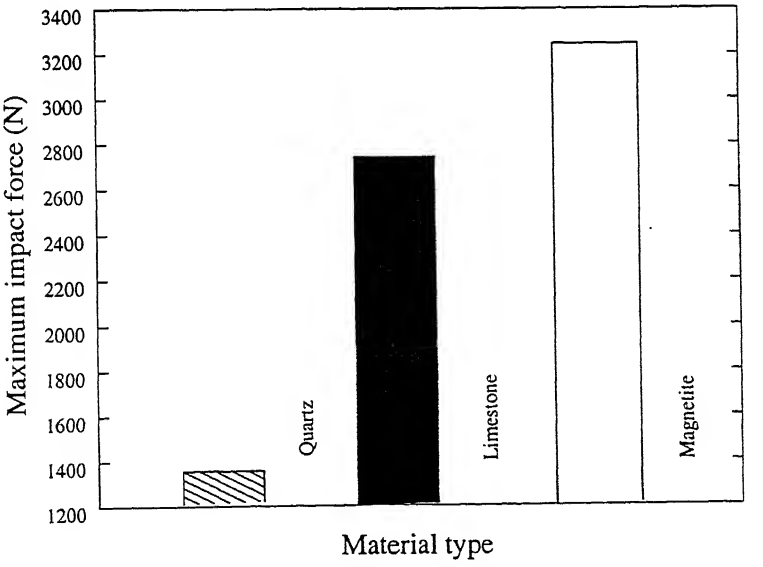


Figure 3.4: Effect of material type on maximum impact force for ball mass 0.252 $kg$ dropped from a height of 0.5 $m$ on 2 layers of particles [13].

## 3.2 Determination of Contact Parameters for Impacts with Particle Layers in Between

Various conditions that have an effect on contact parameters are [15]: ball mass, impact velocity, material to be ground, and number of particle layers. The data gathered from literature depicting the affect of the aforesaid parameters are in the present study used as a basis for contact parameters determination. The non-linear model obtained for the case of metal-metal impact was solved numerically to simulate particle breakage as well. Here, the same procedure as in the case of metal-metal impact, was followed to solve the non-linear equation. Initial guess values of $k$ and $q$ were taken and the model equation (Eqn 2.1) was solved using Fourth Order Runge-Kutta method. The values of the parameters were chosen in such a way that the maximum force and energy loss obtained matched with the experiments. In case of any mismatch, the values of $k$ and $q$ were fine-tuned and the procedure was repeated. The numerical solution provided the contact parameters for the non-linear model for various mill conditions mentioned above. The model was then linearized to get the equivalent linear contact parameters also.

In the following sections, the values of contact parameters obtained are reported and how the above mentioned conditions effect the contact parameters is discussed.

## 3.3 Effect of Impact Velocity or Drop Height of Impacting Ball

It was found that the value of stiffness increased with drop height. The damping term also showed the same trend (see Table 3.1).

Table 3.1: Effect of drop height on contact parameters for ball of mass $0.647\,kg$ and 5 layers of particles.

| Material type | Drop-height (m) | 0.25 | 0.50 | 1.0 |
|---|---|---|---|---|
| Limestone | $k$ | 0.8e8 | 10e8 | 15e8 |
| | $q$ | 0.5e6 | 1.8e6 | 1.78e6 |
| | $k_{eq}$ | 2.2e6 | 2.1e7 | 3.0e7 |
| | $q_{eq}$ | 2740 | 7088 | 12165 |
| Quartz | $k$ | 2.1e8 | 14.1e8 | 32.8e8 |
| | $q$ | 0.33e6 | 1.23e6 | 1.30e6 |
| | $k_{eq}$ | 4.7e6 | 3.5e7 | 6.4e7 |
| | $q_{eq}$ | 1380 | 5411 | 6258 |

It has been shown by Venkatraman and Narayanan [11] that the impact force increases with impact velocity raised to the power 6/5 for ball-ball impact. Therefore, the impact force is expected to increase with drop height. Since, stiffness bears a correspondence with impact force, it also increases with increase in drop height.

It was observed that collision energy increased with velocity of impact. Goldsmith [9] showed that coefficient of restitution decreases with increase in impact velocity (see Appendix B) and consequently with increase in drop height. Damping coefficient being measure of energy loss during collision, increases with decrease in coefficient of restitution and therefore with increase in drop height. Moreover, damping coefficient is also a function of stiffness and increases with increase in stiffness (see Figure 3.5).

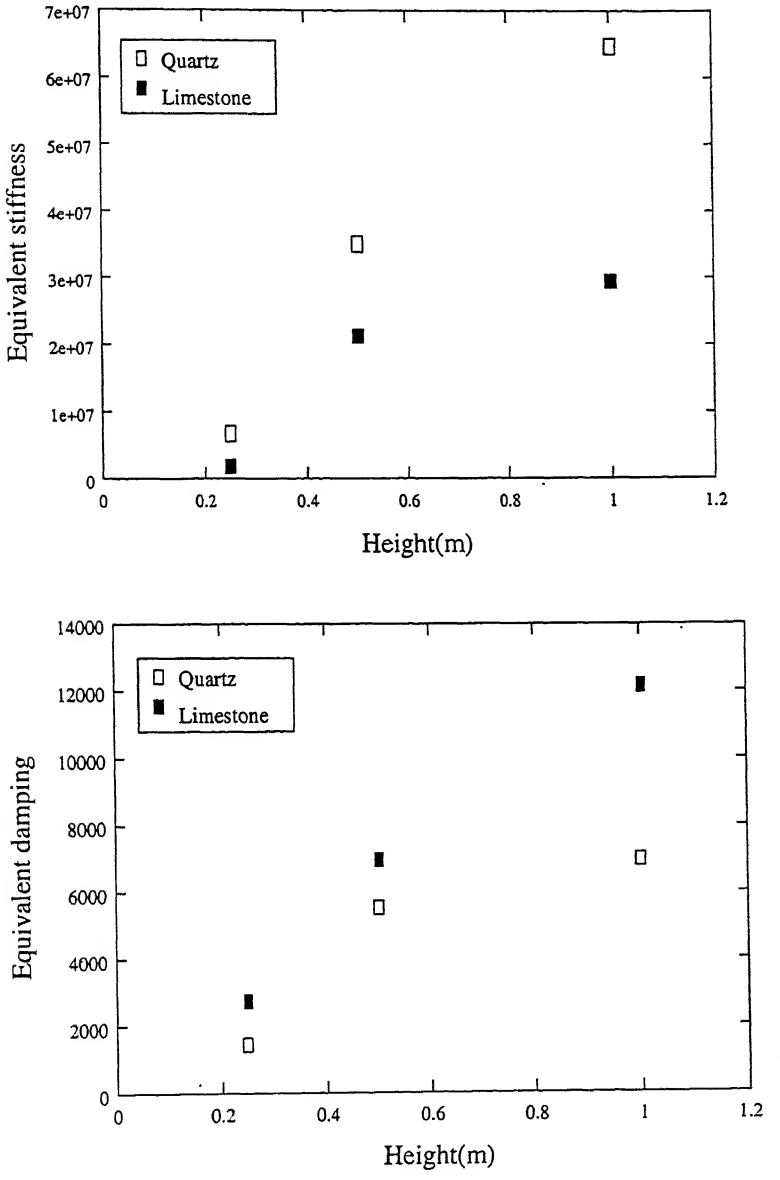


Figure 3.5: Effect of drop height on stiffness and damping values of materials for ball of mass 0.647 $kg$ and 5 layers of particles.

## 3.4 Effect of Number of Particle Layers

It was found that the number of particle layers decreased the contact stiffness and increased the damping coefficient (see Table 3.2).

Table 3.2: Effect of layers of particles on contact parameters for ball of mass 0.647 $Kg$ dropped from the height of 0.25 $m$.

| Material type | | Layers | | |
|---|---|---|---|---|
| | | 2 | 5 | 10 |
| Limestone | $k$ | 1.6e8 | 1.5e8 | 1.4e8 |
| | $q$ | 1.2e6 | 1.23e6 | 1.78e6 |
| | $k_{eq}$ | 3.9e6 | 3.6e6 | 3.2e6 |
| | $q_{eq}$ | 1949 | 2740 | 3310 |
| Quartz | $k$ | 2.38e8 | 2.1e8 | 2.0e8 |
| | $q$ | 0.5e6 | 0.52e6 | 0.6e6 |
| | $k_{eq}$ | 4.5e6 | 4.2e6 | 3.5e6 |
| | $q_{eq}$ | 1000 | 1380 | 1500 |

This is because particles in additional layers increase the cushioning effect on the contact points and reduce the amount of maximum force developed and hence reduce the stiffness.

Also the energy absorbing capacity of layers increase due to the presence of more particles between the balls, thus increasing damping (see Figure 3.6).

## 3.5 Effect of Ball Mass

The ball mass is yet another factor which affects contact parameters. It was found that both stiffness and damping increased with increase in ball mass (see Table 3.3).

It has been reported by Venkataraman and Narayanan [11] that the impact force increases with ball diameter and is proportional to the square of the ball size. This explicitly points to the increase in stiffness with ball mass. Damping

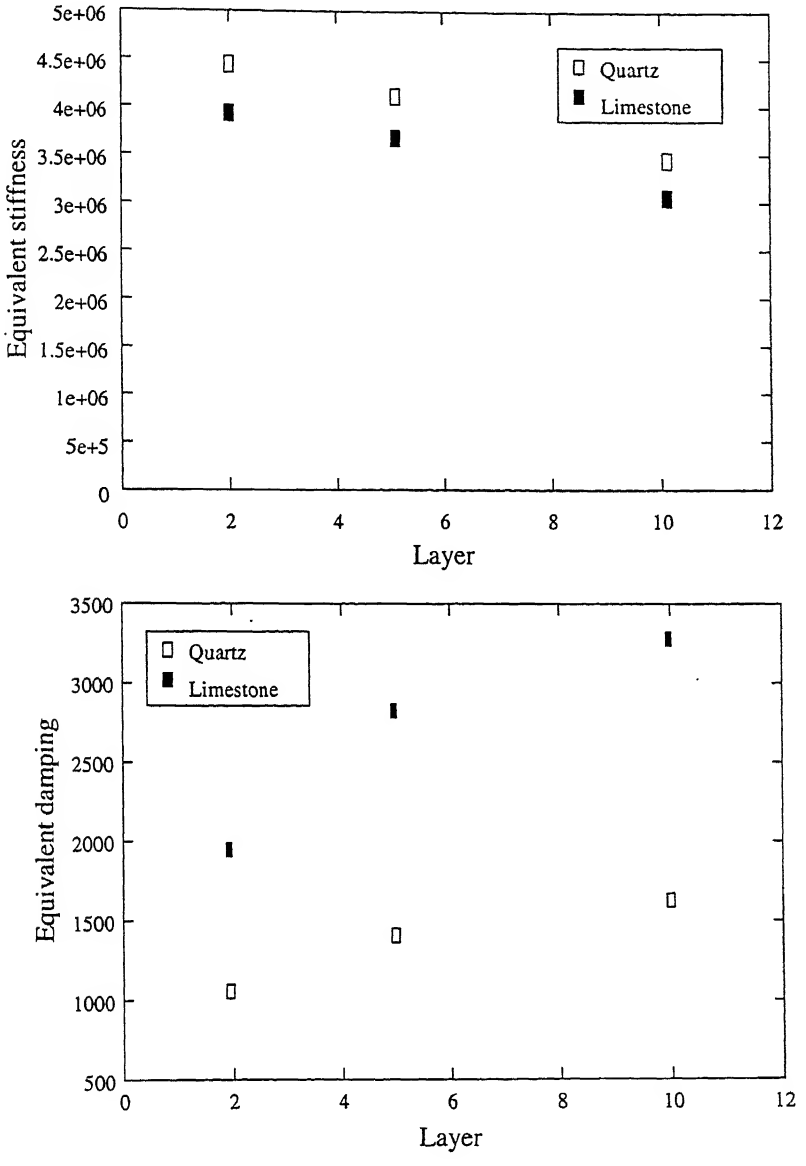


Figure 3.6: Effect of particle layers on stiffness and damping values of materials for ball of mass $0.647\,Kg$ dropped from a height of $0.25\,m$.

Table 3.3: Effect of ball mass on contact parameters for drop height of $0.72\,m$ and 2 layers of magnetite particles.

| | Ball mass (kg) | | |
|---|---|---|---|
| | 0.05 | 0.10 | 0.25 |
| $k$ | 4.7e7 | 1.4e8 | 2.52e8 |
| $q$ | 5e4 | 17e4 | 20e4 |
| $k_{eq}$ | 0.8e6 | 2.8e6 | 4.7e6 |
| $q_{eq}$ | 180 | 530 | 720 |

being a function of mass and as well as a strong function of stiffness, also increases with ball mass (see Figure 3.7).

## 3.6 Effect of Type of Materials to be Ground

It was observed, for three types of materials, the stiffness and damping increased from quartz to limestone and further to magnetite (see Table 3.4).

This trend can be attributed to structural flaws *viz*, pores and cracks. Materials having more flaws break easily *i.e.*, they provide less damping, and have lower strength *i.e.*, they possess lower stiffness (see Figure 3.8).

Table 3.4: Effect of material type on impact parameters for ball of mass 0.647 $Kg$ dropped on 2 layers of particles from a height of 0.25 $m$.

| Material type | Quartz | Limestone | Magnetite |
|---|---|---|---|
| $k$ | 2.0e8 | 2.4e8 | 5e8 |
| $q$ | 1.3e5 | 4.0e5 | 5.0e5 |
| $k_{eq}$ | 3.2e6 | 4.0e6 | 7.7e6 |
| $q_{eq}$ | 509 | 1249 | 1897 |

## 3.7 Determination of Coefficient of Restitution

Coefficient of restitution is defined as a ratio between velocity just after impact, $v_a$ and velocity just before impact, $v_b$. Mathematically, coefficient of restitution is given as

$$e = -\frac{v_a}{v_b} \tag{3.1}$$

Calculation of coefficient of restitution $e$ is of utmost importance because it is one of the input parameters required in simulation . In fact, a DEM code [18] is

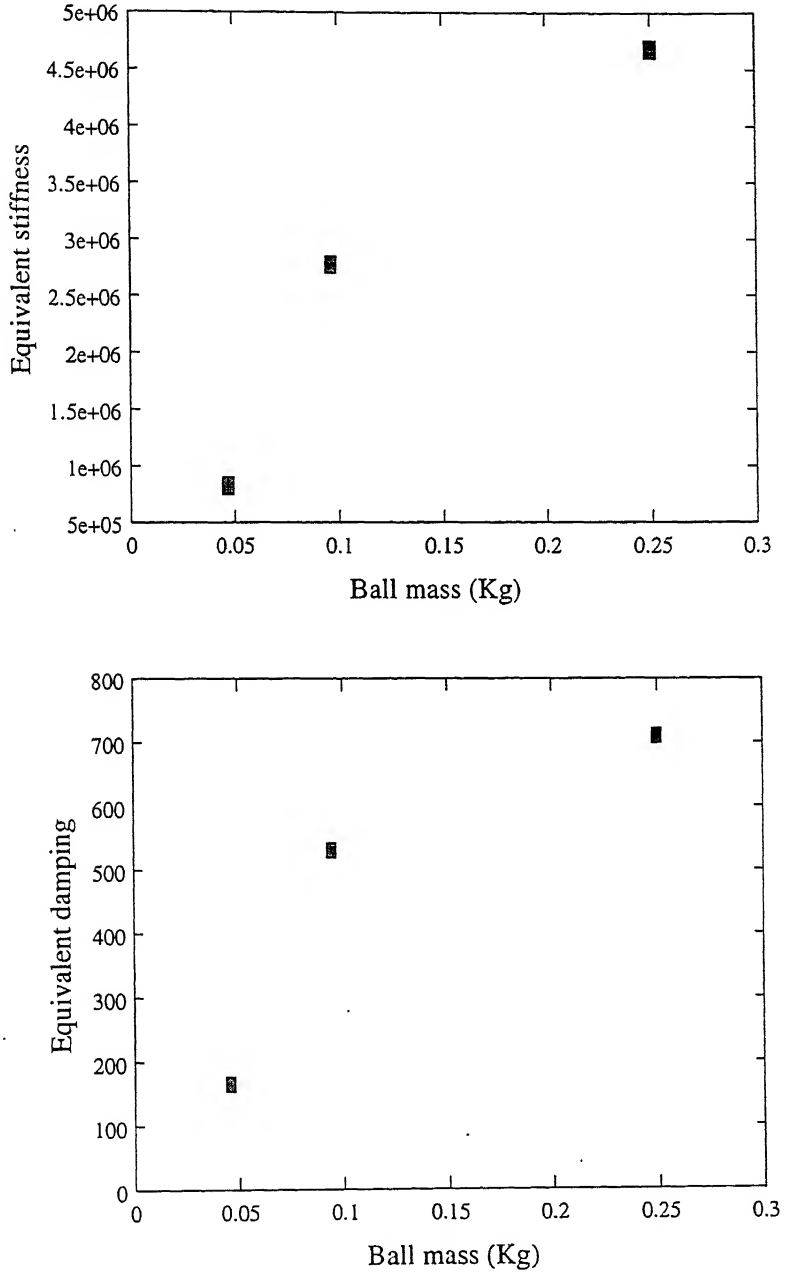


Figure 3.7: Effect of ball mass on contact parameters for drop height of 0.72 $m$ and 2 layers of magnetite particles.

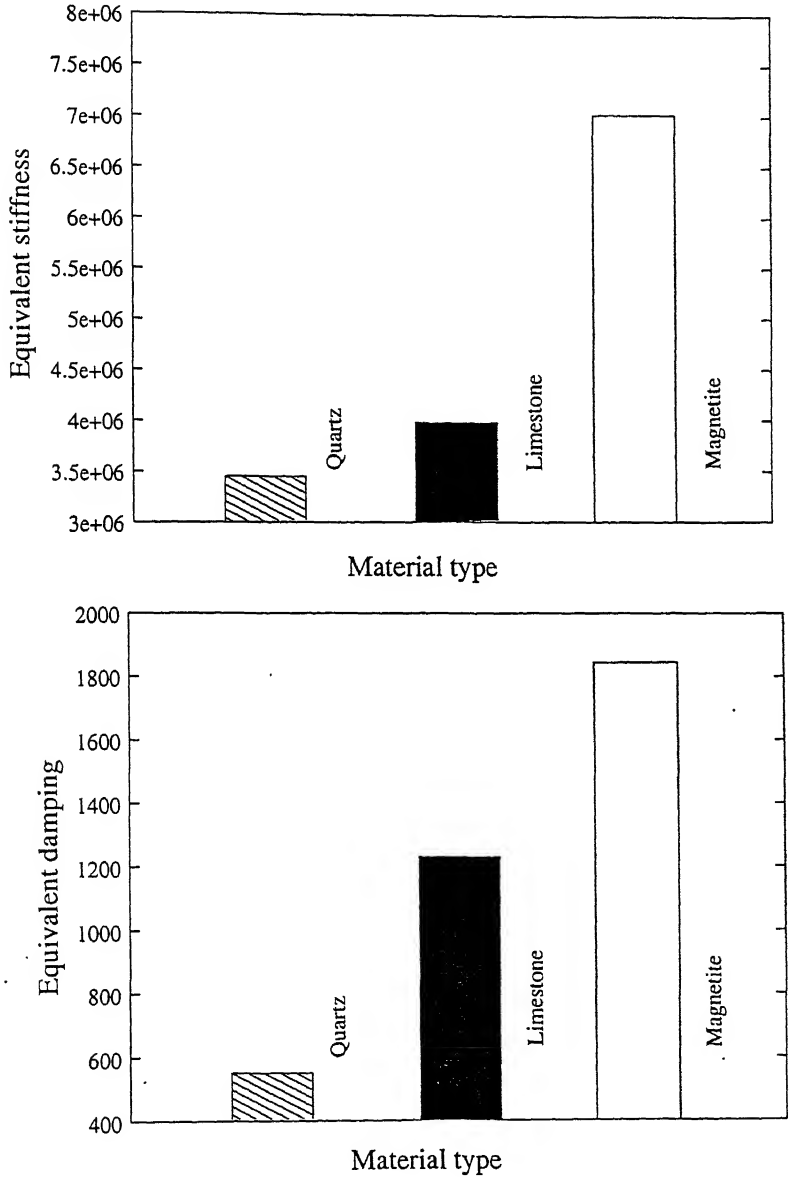


Figure 3.8: Effect of material type on contact parameters for ball of mass $0.647 Kg$ dropped on 2 layers of particles from a height of $0.25\ m$.

available which takes material properties *viz.*, stiffness, coefficient of restitution and coefficient of friction as input parameters. The values of parameters obtained by non-linear and equivalent linearized methods were used to calculate coefficient of restitution. The non-linear and linearized model were solved numerically using the corresponding non-linear and linearized stiffness and damping parameters. The velocity of ball just before impact was set at $2.4\,m/sec$. Impact velocity of this magnitude is encountered in ball mills having diameter of $0.545\,m$ where the ball is dropping from the mill centre vertically downwards on the mill wall. The impact process was assumed to be over when the impact force returned back to zero. Then the velocity just after impact was calculated. The ratio of final velocity to initial velocity with the sign changed gave the value of coefficient of restitution[1]. The following plots (see Figure 3.9 and Figure 3.10) show the variation of coefficient of restitution with damping for non-linear and equivalent linearized models.

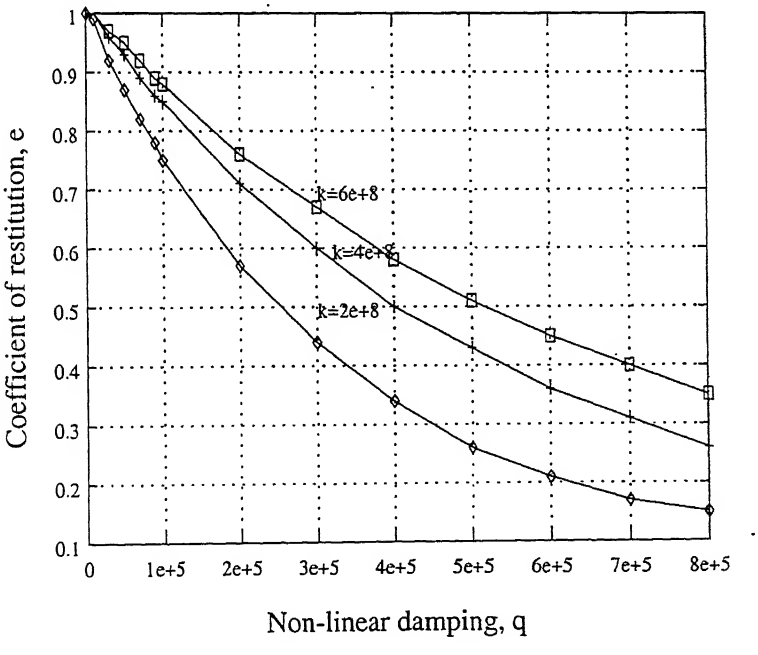


Figure 3.9: Variation of coefficient of restitution with damping constant $q$ for ball of mass $0.647\,kg$ having impact velocity $2.4\,m/sec$ (non-linear model).

[1]For linear model it is possible to arrive at the analytical solution for coefficient of restitution, for derivation see Appendix B.

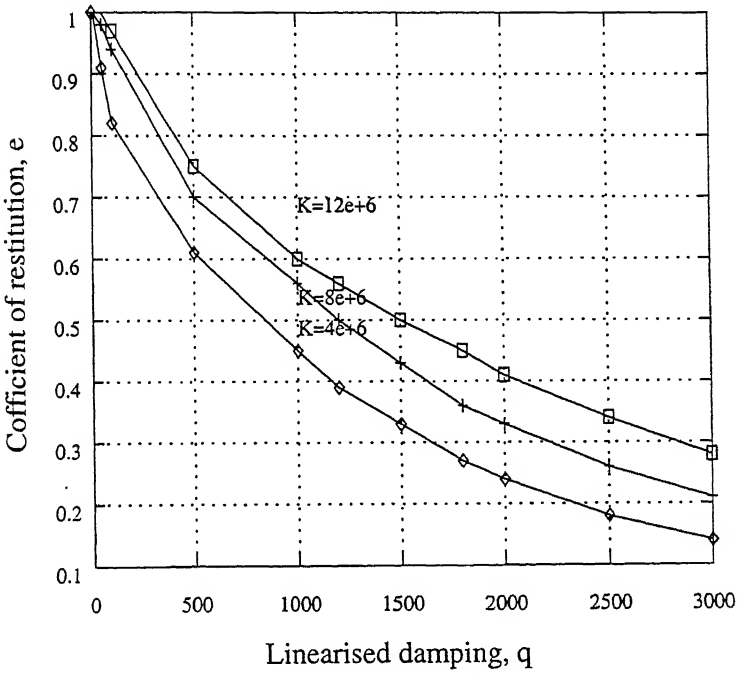


Figure 3.10: Variation of coefficient of restitution $e$ with damping constant $q$ for ball of mass $0.647\,kg$ having impact velocity $2.4\,m/sec$ (equivalent linearized model).

# Chapter 4

# Simulation of a Ball Mill by DEM

In this chapter a 54.5 $cm$ diameter and 30.8 $cm$ long ball mill is simulated by using a DEM based simulator [18]. Two types of contact models were used in the simulation *viz.*, linear and non-linear. However, the contact parameters in the case of a linear model were changed to incorporate the equivalent parameters extracted from the non-linear model. Several simulations were carried out and the computed power draw was compared with the corresponding experimental data.

## 4.1 Mill Set-up for Simulation

In this section, a laboratory size ball mill is considered to predict the power draw as a function of mill speed. This can be easily done by means of a DEM based simulator that tracks the motion of balls in all three directions. In order to assess the accuracy of the prediction power draw, available experimental data on a 54.5 $cm \times 30.4\,cm$ ball mill is considered. These data were published by Liddell and Moys [?], where the authors claim an accuracy of 0.5 percent in their data. Thus, these data are found most suitable for comparison purpose.

A mill similar to that used by Liddell and Moys is considered for simulation. It

is a smooth mill without lifters. The grinding media is made up of graded charge of $0.029\,m$, $0.04\,m$, and $0.054\,m$ diameter balls having masses $0.096\,kg$, $0.252\,kg$, and $0.647\,kg$ respectively. To ensure mill filling of approximately 40%, 324 balls were generated randomly. In addition, the total load was maintained at $140\,kg$ by slightly increasing the density of the balls up to $8400\,kg/m^3$.

The DEM based simulator [18], was fed with the above data and trial runs were carried out in SUN-Ultra450 machine. Figure 4.1 shows snapshots (front view) of the mill rotating at 60 % and 95 % of critical speed. The critical speed of mill is $6.05\,radians/sec.$

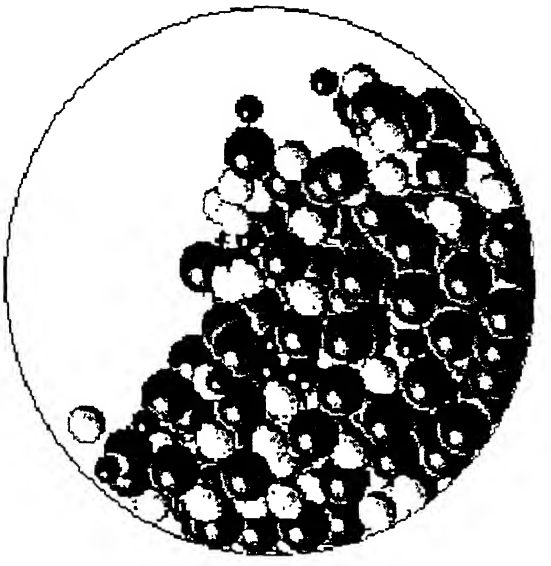

(a)

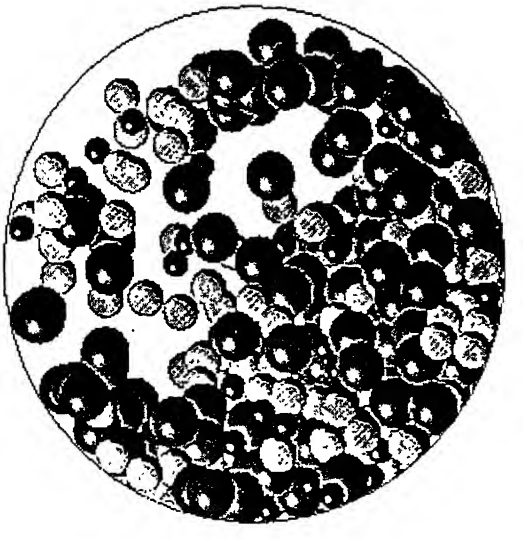

(b)

Figure 4.1: Figures showing snapshots (front view) of the mill for (a) 60 % and (b) 95 % of critical speed.

## 4.2 Mill Simulation

There are basically three contact stiffness models that are tested through the following numerical simulations. These are

- Linear model

$$F = kx \tag{4.1}$$

- Equivalent linearized model

$$F = k_{eq}x \tag{4.2}$$

- Non-linear model

$$F = kx^{1.6} \tag{4.3}$$

It is clear that all the three models are parameter dependent. In particular, the stiffness and the coefficient of restitution by and large decide the model response. Thus, at the very outset, the model parameters used in the respective simulations are shown in Table 4.1. This table shows the values of parameters that are used in the simulation such as stiffness, damping, coefficient of restitution, and coefficient of friction. In the same table, the critical time-step required for the DEM simulation is also shown. These data are obtained as per the procedure described in Chapters 2 and 3. Briefly, the stiffness value in the case of a linear model was obtained by considering the initial slope of experimental force-deformation curve. In the case of non-linear model, the value of stiffness was directly extracted from the model (Equation 2.1) that matched the UFLC data. The equivalent param-

eters were then extracted from the non-linear model by applying the technique called equivalent linearisation.

Table 4.1: Data used for simulation.

| Model type | Linear | Equivalent linearized | Non-linear |
|---|---|---|---|
| Normal stiffness $k$ | 4.0e5 | 11.3e6 | 5.53e8 |
| Shear stiffness $k_s$ | 3.0e5 | 7.53e6 | 3.69e8 |
| Coefficient of restitution $e$ | 0.45 | 0.31 | 0.42 |
| Coefficient of friction $\mu$ | 0.90 | 0.90 | 0.2 |
| Critical time-step $\Delta t\,(sec)$ | 2.09e-4 | 3.9e-5 | 5.57e-6 |

At first, the linear contact model was considered. The $0.545\,m$ diameter mill was simulated by using the DEM based simulator where the contact model was appropriately set. At the end of the simulation, the power draw of the mill corresponding to the set of operating conditions was noted. To begin with, simulations were carried out for different values of coefficient of friction. The results obtained are shown in Table A.5 in Appendix A. This was done in order to get the most accurate power draw for a single value of coefficient of friction. It was found that for a value of coefficient of restitution of 0.9, the maximum power draw predicted by the model was 93 % of the experimental maximum power draw. Finally, several simulations were conducted to establish the variation in power draw of the mill with its speed. All the simulations at each mill speed were carried out for three revolutions and an average power draw was considered for comparison purpose.

Next, the non-linear and equivalent linearized models were tested in a similar manner. Since, the linear model predicted power draw close to 93 % for coefficient of friction 0.9, it was decided to use the same value of coefficient of friction for equivalent linearized model. Table 4.2 shows the power draw predicted by using the linear model, equivalent linearized model and the non-linear model for different mill speeds. For the purpose of comparison the experimental data is also presented

in the same table. The following observations are made from the table:

- It is seen from the table that the non- linear model could not predict the experimentally observed power draw.

Table 4.2: Comparison between simulated power draw results with the experimental power draw.

| Mill speed (% of critical) | Power draw ($W$) | | | |
|---|---|---|---|---|
| | Experimental | Linear model $\mu = 0.90$ | Equivalent linearized model $\mu = 0.90$ | Non-linear model $\mu = 0.20$ |
| 50 | 390 | 384.2 | 400.5 | 547.5 |
| 60 | 490 | 475.9 | 488.6 | 650.0 |
| 70 | 590 | 546.0 | 579.3 | 753.7 |
| 75 | 640 | 574.8 | 627.7 | 854.2 |
| 80 | 683 | 610.4 | 668.5 | 1031.4 |
| 90 | 700 | 651.1 | 710.2 | 1533.9 |
| 95 | 683 | 630.6 | 679.0 | 968.8 |

- The power draw predicted by equivalent linearized model agrees quite well with the experimental power draw.

- Between the three models, the equivalent linearized model is found to be the most accurate one.

The numerical data is also compared against the experimental data in Figure 4.2. It is seen from this figure that all three models show the same trend in the variation in power draw *i.e.*, there exists a maxima in the power draw corresponding to a particular mill speed. Interestingly, all three model correctly predict this speed at which the power draw is maximum. However, the non-linear model could not match the power draw. It is believed that incorporation of the non-linear model into the 3-D DEM code has to be done more carefully.

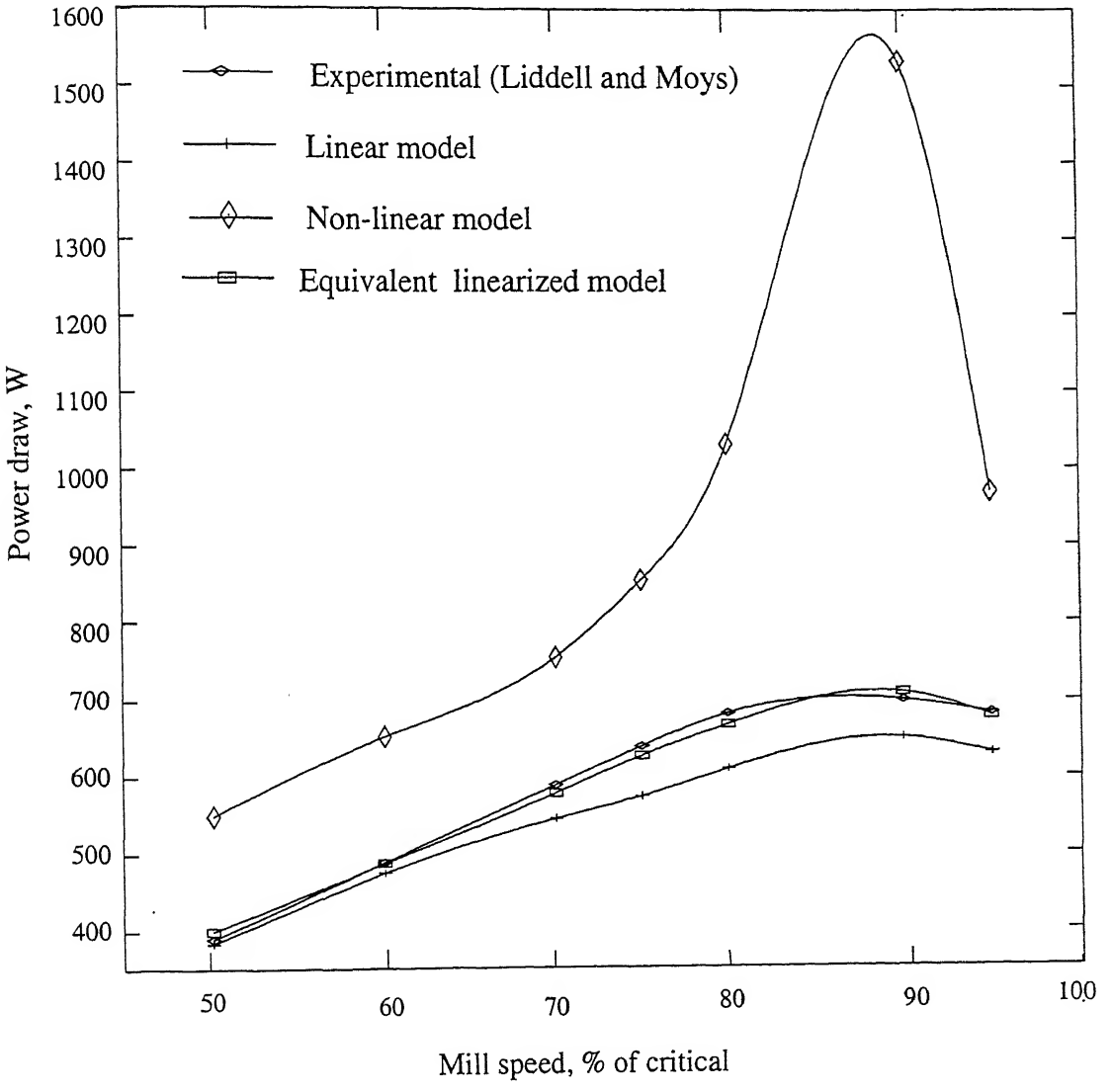


Figure 4.2: Comparison between linear model, equivalent model and experimental results.

# Chapter 5

# Summary and Discussions

The discrete element method (DEM) has become a powerful tool for systematic analysis of the charge behavior in many of the mineral processing units such as ball mill and jigs. However, it suffers from the criticism that the discrete element models are highly parameter dependent and there is no unique way of establishing these parameters. This research work was undertaken to dispel this state of affairs by establishing a procedure to correctly determine the parameters *viz.*, contact stiffness, damping, etc., while keeping the numerical and computational expense manageable.

At first, the available experimental data on drop ball tests using a ultra fast load cell (UFLC) is considered. These data show the deformation behavior of the contact when a steel ball is dropped onto a steel anvil. Analysis of these type of metal-metal impacts reveal that a non-linear contact model adequately represent the contact behavior. The contact model adopted was of the following form:

$$m\ddot{x} + qx^{0.8}\dot{x} + kx^{1.6} = 0 \tag{5.1}$$

where, $k$ is stiffness parameter and $q$ is damping parameter. The parameters

involved in this model are extracted after matching the model response with the experimental data. These parameters allowed for the calculation of the energy involved during a given impact. This formed the basis for assessing the suitability of a particular contact model for the impact problem under investigation.

The force-displacement behavior obtained during a collision (metal-metal) is modeled by using a non-linear as well as a linear contact model. It was found that the non-linear model best described the experimental data. In particular, the energy expended during the collision was very accurately predicted by using the non-linear model. However, the material stiffness as a parameter in the model turned out to be of the order of $10^{10}\,N/m^{1.6}$. This has serious ramification when this value is used in a discrete element model where the goal is to simulate the behavior of not just a single ball but thousands of balls. A large value of contact stiffness reduces the time-step of integration adding to the computational expense.

In order to circumvent the above problem, a new approach is taken to transform the non-linear contact behavior to the most appropriate linear behavior in a formal sense. In this approach, the non-linear model is converted into its equivalent linear form using a equivalent linearisation technique. This method provided a linear stiffness value of $10^8\,N/m$ which is two orders in magnitude lower than that of the corresponding non-linear stiffness parameter. Thus, the computational time significantly lowered by adopting the equivalent linearisation technique.

In the foregoing, only metal-metal type collision problems are considered. But, it is realized that real ball mill simulation would involve particles that are to be ground. Under these circumstances, the contact model must incorporate material parameters that will take into account the presence of particles between colliding balls. Experimental data on drop ball test incorporating particle layers are gathered from the literature. Analysis of these data show that a contact stiffness of $10^6\,N/m$ sufficiently describes the contact behavior. This value of stiffness further

reduces the time-step in comparison to metal-metal collision problem.

The performance of the equivalent linearized model is assessed by incorporating it into a generalized DEM software. A laboratory size mill of diameter $0.545\,m$ and length $0.308\,m$ was simulated. Three contact models of linear, equivalent linearized, and non-linear type were considered. Three types of balls were used in the simulation for which contact parameters were available. The ball mill was simulated to obtain the variation in power draw with mill speed. It was found while comparing with the available experimental data on a similar ball mill that equivalent linearized model predicted the power draw most accurately.

The equivalent linearized model, although, is able to predict the power draw accurately, it fails to give the correct force-deformation and force-time histories. It is therefore suggested to use a displacement term in the relationship for the damping force so that initially when the deformation is zero the net force is also made equal to zero.

# Appendix A

# Experimental Data Used in the Present Study

## A.1 Ultra Fast Load Cell Data Tables

The tables below (Table A.1 through Table A.4) depict the data collected by UFLC experiments which were used for parametric analyses.

Table A.1: UFLC impact data with no particle layers in between.

| Experiment No. | 1 | 2 | 3 |
|---|---|---|---|
| Particle Layer | 0 | 0 | 0 |
| Ball Mass ($kg$) | 0.096 | 0.647 | 0.252 |
| Ball Height ($m$) | 0.30 | 0.30 | 0.30 |
| Impact Velocity ($m/sec$) | 2.4 | 2.4 | 2.4 |
| Input Energy ($J$) | 0.28 | 1.86 | 0.73 |
| Consumed Energy ($J$) | 0.20 | 1.08 | 0.47 |
| Maximum Force ($N$) | 8109 | 26000 | 15025 |
| Maximum Displacement ($mm$) | 0.075 | 0.136 | 0.107 |
| Maximum Time ($\mu sec$) | 78 | 154 | 116 |

Table A.2: UFLC impact data on limestone.

| Impact Condition | Particle Layers | Ball Mass ($kg$) | Ball Height ($m$) | Impact Velocity ($m/sec$) | Input Energy ($J$) | Consumed Energy ($J$) | Maximum Force ($N$) | Maximum Displacement ($mm$) |
|---|---|---|---|---|---|---|---|---|
| Ball/Flat | 2 | 0.647 | 0.15 | 1.70 | 0.93 | 0.92 | 1219 | 2.16 |
| | | | 0.25 | 2.19 | 1.55 | 1.52 | 2405 | 2.39 |
| | | | 0.50 | 3.10 | 3.11 | 2.95 | 7496 | 2.78 |
| | | | 1.0 | 4.38 | 6.20 | 5.58 | 17361 | 2.50 |
| | 5 | | 0.25 | 2.19 | 1.55 | 1.52 | 2366 | 3.66 |
| | | | 0.50 | 3.10 | 3.11 | 2.92 | 8432 | 2.42 |
| | | | 1.0 | 4.38 | 6.20 | 5.89 | 11277 | 7.90 |
| | 10 | | 0.25 | 2.19 | 1.55 | 1.52 | 2587 | 3.69 |
| | | | 1.0 | 4.38 | 6.20 | 5.83 | 13430 | 4.37 |
| | 3 | 0.252 | 0.25 | 2.07 | 0.54 | 0.47 | 370 | 2.89 |
| | | | 0.50 | 2.92 | 1.08 | 0.98 | 601 | 4.5 |
| | | | 0.75 | 3.58 | 1.62 | 1.48 | 1065 | 5.08 |
| | | | 1.0 | 4.13 | 2.16 | 2.00 | 1798 | 4.44 |
| Ball/Ball | 2 | 0.647 | 0.15 | 1.70 | 0.93 | 0.92 | 2354 | 3.16 |
| | | | 0.25 | 2.19 | 1.55 | 1.44 | 5367 | 3.38 |
| | | | 0.50 | 3.10 | 3.11 | 2.71 | 11850 | 3.00 |
| | 5 | | 0.15 | 1.70 | 0.93 | 0.88 | 5037 | 2.01 |
| | | | 0.25 | 2.19 | 1.55 | 1.39 | 7783 | 1.74 |
| | | | 0.50 | 3.10 | 3.11 | 2.61 | 15835 | 1.63 |
| | 1 | 0.252 | 0.15 | 1.70 | 0.36 | 0.36 | 400 | 3.10 |
| | | | 0.25 | 2.19 | 0.61 | 0.59 | 1131 | 3.42 |
| | | | 0.50 | 3.10 | 1.21 | 1.17 | 3228 | 3.24 |

Table A.3: UFLC impact data on quartz.

| Impact Condition | Particle Layers | Ball Mass ($Kg$) | Ball Height ($m$) | Impact Velocity ($m/sec$) | Input Energy ($J$) | Consumed Energy ($J$) | Maximum Force ($N$) | Maximum Displacement ($mm$) |
|---|---|---|---|---|---|---|---|---|
| Ball/Flat | 5 | 0.647 | 0.25 | 2.07 | 1.38 | 1.27 | 2802 | 2.61 |
| | | | 0.50 | 2.92 | 2.76 | 2.62 | 8952 | 2.78 |
| | | | 1.00 | 4.13 | 5.52 | 5.13 | 18923 | 2.10 |
| | 10 | | 0.25 | 2.07 | 1.38 | 1.25 | 2349 | 2.81 |
| | | | 0.5 | 2.92 | 2.76 | 2.62 | 7151 | 3.00 |
| | | | 1.00 | 4.13 | 5.52 | 5.13 | 15703 | 2.90 |
| | 3 | 0.252 | 0.50 | 2.92 | 1.08 | 1.02 | 1339 | 4.47 |
| | | | 0.75 | 3.58 | 1.62 | 1.53 | 2190 | 4.29 |
| | | | 1.00 | 4.13 | 2.16 | 2.05 | 4203 | 4.54 |
| Ball/Ball | 5 | 0.647 | 0.25 | 2.07 | 1.38 | 1.24 | 10951 | 0.69 |
| | | | 0.50 | 2.92 | 2.76 | 2.46 | 17020 | 0.82 |
| | | | 1.00 | 4.13 | 5.52 | 4.75 | 27722 | 0.85 |
| | 10 | | 0.25 | 2.07 | 1.38 | 1.27 | 9275 | 0.69 |
| | | | 0.50 | 2.92 | 2.76 | 2.43 | 17939 | 0.71 |
| | | | 1.00 | 4.13 | 5.52 | 4.80 | 26795 | 0.8 |

Table A.4: ULFC impact data on magnetite.

| Particle Layer | Ball Mass ($kg$) | Ball Height ($m$) | Impact Velocity ($m/sec$) | Input Energy ($J$) | Consumed Energy ($J$) | Maximum Force ($N$) | Maximum Displacement ($mm$) |
|---|---|---|---|---|---|---|---|
| 2 | 0.096 | 0.33 | 2.52 | 0.31 | 0.29 | 583 | 2.52 |
| | | 0.67 | 3.59 | 0.62 | 0.61 | 1463 | 2.29 |
| | | 1.34 | 5.07 | 1.24 | 1.22 | 3087 | 2.91 |
| | 0.252 | 0.13 | 1.58 | 0.31 | 0.27 | 463 | 1.77 |
| | | 0.26 | 2.24 | 0.63 | 0.60 | 977 | 2.06 |
| | | 0.51 | 3.13 | 1.24 | 1.22 | 2715 | 2.08 |
| | 0.647 | 0.10 | 1.39 | 0.62 | 0.59 | 1145 | 2.05 |
| | | 0.20 | 1.96 | 1.24 | 1.20 | 3709 | 1.41 |

## A.2 Mill Simulation Data Tables

Table A.5: Power predicted by linear model for different values of coefficient of friction.

| | Power draw ($W$) | | | |
|---|---|---|---|---|
| Mill speed | Coefficient of friction | | | |
| % of critical | 0.3 | 0.5 | 0.7 | 0.9 |
| 60 | 255.0 | 332.7 | 413.6 | 475.9 |
| 70 | 298.9 | 391.4 | 480.7 | 546.0 |
| 75 | 320.3 | 418.5 | 513.3 | 574.8 |
| 80 | 346.2 | 445.5 | 534.8 | 610.4 |
| 90 | 368.3 | 467.6 | 567.5 | 651.1 |
| 95 | 354.8 | 496.3 | 557.1 | 630.6 |

# Appendix B

# Important Derivations and Relations

## B.1 Derivation of Damping Constant for Linear Model

The equation of motion for the oscillating system consisting of a mass, spring and a dashpot is

$$m\ddot{x} + q\dot{x} + kx = 0 \tag{B.1}$$

The solution [16] of this equation under the initial condition that $x = 0$ and $\dot{x} = v_i$ at $t = 0$ is given by

$$x = \left(\frac{v_i}{\eta}\right) \sin(\eta t) \exp(-\gamma\omega_0 t) \tag{B.2}$$

$$\dot{x} = \left(\frac{v_i}{\eta}\right) \{\eta \cos(\eta t) - \gamma\omega_0 \sin(\eta t)\} \exp(-\gamma\omega_0 t) \tag{B.3}$$

where

$$\omega_0 = \sqrt{k/m} \tag{B.4}$$

$$\gamma = \frac{q}{2\sqrt{mk}} \tag{B.5}$$

$$\eta = \omega_0\sqrt{1-\gamma^2} \tag{B.6}$$

The oscillation period of this system is $2\pi/\eta$. A particle colliding with another particle at the time $t = 0$ detaches at time $t = \pi/\eta$. The velocity at the time $t = \pi/\eta$ is given by

$$v_0 = \dot{x}\mid_{t=\pi/\eta} = -v_i \exp(\gamma\omega_0\pi/\eta) \tag{B.7}$$

Therefore, the coefficient of restitution becomes

$$e = -v_0/v_i = \exp(\gamma\omega_0\pi/\eta) \tag{B.8}$$

If the coefficient of restitution is regarded as a constant empirical parameter (it depends on impact velocity, in fact), the damping coefficient may be determined from the above equations. Consequently, the damping coefficient is given by

$$q = -2\ln e\sqrt{\frac{mk}{\ln^2 e + \pi^2}} \tag{B.9}$$

where $m$ is the ball mass, $k$ is the contact stiffness, $t$ is he impact time, and $x$ is the ball deformation.

## B.2 Relation Between Coefficient of Restitution and Impact Velocity

It was observed by Goldsmith [9] that the magnitude of coefficient of restitution decreased monotonously from unity with increasing impact velocity (Figure B.1). Also, the reduction in value of coefficient of restitution was greater than can be justified by the loss of energy due to damping. This feature contradicts the basic assumption of the Hertz theory of contact regarding perfect elasticity of process in which in absence of damping force the coefficient of restitution becomes unity. Therefore, it is revealed that apart from energy loss due to damping, there is some extra loss of energy due to plastic deformation of balls. It follows that the model

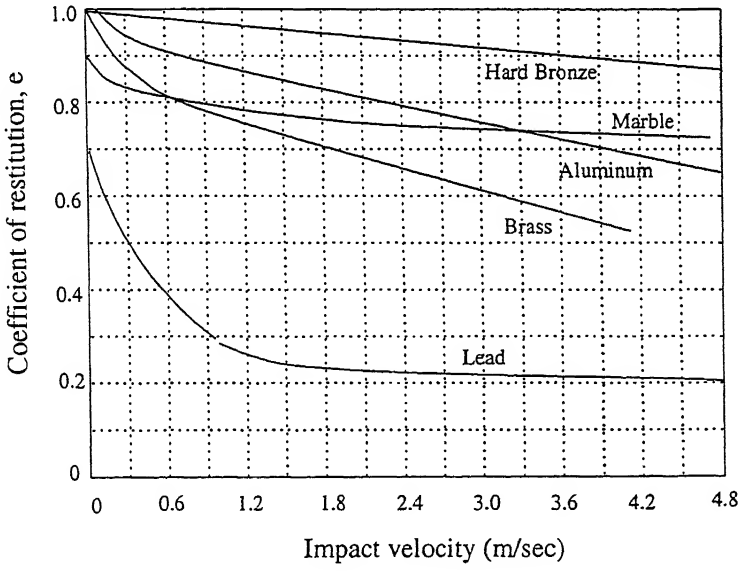


Figure B.1: Coefficient of restitution as a function of impact velocity for spheres of same size but different materials, after Goldsmith [9].

developed in the present work requires some modifications to take into account the permanent deformation of balls by taking into consideration the strain-rate effects in the material behavior.

# References


[1] P.A. Cundall and O.D.I.. Strack, *A Discrete Numerical Model for Granular Assemblies,* Geotechnique, Vol. 29 pp 47-64, 1974 .

[2] R. Dobry and T.T. Ng, *Discrete Modeling of Stress-Strain Behavior of Granular Media at Small and Large Strains*, Paper presented at the 1st International Conference on Discrete Element Modeling, Colorado, 1989

[3] G.G.W. Mustoe, M. Henriksen, and H.P. Huttelmaier, *Proceedings of the 1st U.S. Conference on Discrete Element Methods*, Colorado, 1989

[4] R. Zhang, G.C.W. Mustoe and K.R. Nelson, *Simulation of Hydraulic Phenomena Using Discrete Element Method,* Proceedings of 2nd International Conference on Discrete Element Method (DEM), The Massachusetts Institute of Technology, March 18-19 , pp 189-200 , 1993.

[5] Y. Tsuji, T. Kawaguchi and T. Tanaka, *Discrete Particle Simulation of Two-Dimensional Fluidized Bed*, Powder Technology, Vol. 77 pp 79-87, 1993.

[6] D. Zhang and W.J. Whiten, *The Calculation of Contact Forces Between Particles Using Spring and Damping Models,* Powder Technology, 88 (1996) 59-64.

[7] Engel A. Peter, *Impact Wear of Materials,* Elsevier Scientific Publishing Co., Amsterdam, pp 29-59, 1970.

[8] Y. Tsuji, T. Tanaka and T. Ishida, *Lagrangian Numerical Simulation of Plug Flow of Cohesionless Particles in a Horizontal Pipe,* Powder Technology, Vol. 71, pp 239-250, 1992.

[9] W. Goldsmith, *Impact. The Theory and Physical Behavior of Colliding Solids,* Edward Arnold, London (1967).

[10] R.P. King and F. Bourgeois, *Measurement of Fracture Energy During Single-Particle Fracture,* Minerals Engineering, Vol. 6 No. 4 (1993) 353-367.

[11] K.S. Venkataraman and K.S. Narayanan, *Energetics of Collision Between Grinding Media in Ball Mills and Mechanochemical Effects,* Powder Technology, Vol. 96, pp 190-201, 1998.

[12] John M. Ting, Brent T. Corkum, Claudia R. Kauffman and Carlo Greco, *Discrete Numerical Modeling of Soil,* Department of Civil Engineering, University of Toronto, June 1987.

[13] Andreas Höfler, *Fundamental Breakage Studies of Mineral Particles with an Ultrafast Load Cell Device,* Ph. D Thesis, University of Utah, 1991.

[14] B. K. Mishra, *Study of Media Mechanics in Tumbling Mills by the Discrete Element Methòd, Ph.D. Thesis,* University of Utah, USA, 1991.

[15] B.K. Mishra and R.K. Rajamani, *The Discrete Element Method for the Simulation of Ball Mill,* Applied Mathematical Modeling , Vol. 16 November , 1992.

[16] B.T. Corkum and J. M. Ting, *The Discrete Element Method in Geotechnical Engineering,* Paper presented at the 3rd International Conference on Computing in Civil Engineering Vancouver, Canada, August, 1988.

[17] B. K. Mishra and R. K. Rajamani, *Program Thrddball,* Comminution Center University of Utah, 1993.

[18] K.S. Liddell and M.H. Moys, *The Effects of Mill Speed and Filling on the Behavior of the Load in a Rotary Grinding Mill*, Journal of South African Institute of Mining and Metallurgy, Vol.88, No.2, pp. 49-57, February 1988.